Int. J. Heat Mass Transfer. Vol. 9, pp. 995–1020. Pergamon Press 1966. Printed in Great Britain

THE MECHANISM OF NUCLEATE BOILING IN PURE LIQUIDS AND IN BINARY MIXTURES—PART I

S. J. D. VAN STRALEN.

Heat Transfer Section, Technological University, Eindhoven, The Netherlands

(*Received* 14 *January* 1966)

Abstract—The author's modification of the theories by van Wijk, Vos and van Stralen, by Scriven and by Bruijn, concerning the growth rate of free spherical vapour bubbles in uniformly superheated binary mixtures is extended to the more complex cases of bubbles generated on a heating surface and of time-dependent liquid superheating, leading to a new description of the mechanism of nucleate boiling.

The heat flow to the bubble required for vaporization during rapid initial bubble growth has been derived from the excess enthalpy of the equivalent conduction layer at the heating surface. This thermal boundary layer is periodically pushed away from the wall due to the generation of succeeding bubbles on nuclei. The behaviour of the uniform superheating of the fluctuating microlayer has been established similar to a relaxation phenomenon.

The various interpretations of rapid temperature dips, occurring both in nucleate boiling and film boiling, at the heating surface due to initial vapour formation have been discussed and the proposed mechanism has also been checked with schlieren photographs taken from the literature.

The experimental growth of bubbles adhering to a platinum heating wire in water, and in water–methylethylketone and water–1-butanol mixtures, is in quantitative agreement with the new theory.

NOMENCLATURE

a, $k/\rho_1 c$, (liquid) thermal diffusivity [m^2/s];

A, area of surface [m^2];

A_1, $4\pi R^2$, area of spherical bubble surface [m^2];

A_2, $4\pi b R^2$, area of spherical heating segment surrounding a part of the bubble boundary [m^2];

b, $eR_{1,e}/C_1\vartheta_0 u_{1,e}$, dimensionless bubble growth parameter;

b_1, corrected dimensionless bubble growth parameter;

b^*, dimensionless microlayer parameter for a spherical segment; $b^* = b$ for a sphere;

B, $(\frac{1}{2})(1 + \cos\alpha)$ = dimensionless wetting parameter for a spherical segment;

c, (liquid) specific heat at constant pressure [J/kg degC];

C, heat capacity of relaxation microlayer [J/degC];

C_1, $= R/\vartheta t^{\frac{1}{2}}$, bubble growth constant, for relatively large liquid superheatings, $C_1 = 24 \times 10^{-4}$ for water, $C_1 = 6 \times 10^{-4}$ for 4·1 wt. % methylethylketone, $C_1 = 18 \times 10^{-4}$ for 1·5 wt. % 1-butanol and $C_1 = 21 \times 10^{-4}$ for 6·0 wt. % 1-butanol, all at atmospheric pressure [$m/s^{\frac{1}{2}}$ degC];

C_2, $= R/t^{\frac{1}{2}}$, bubble growth factor [$m/s^{\frac{1}{2}}$];

d, instantaneous thickness of relaxation microlayer, or of equivalent conduction layer [μ or m];

D, mass diffusivity of more volatile component in less volatile component [m^2/s];

D_w, diameter of heating wire [m];

†Doctor of Physics, Principal Research Officer.

D_1, $= \vartheta_0$, constant of integration [degC];
D_2, $= -\vartheta_0$, constant of integration [degC];
D_3, $= 4\pi b^3 C_1^3 \vartheta_0^2 \rho_2 l/\rho_1 c$, constant [$m^3/s^{\frac{1}{2}}$];
f_1, 1, or $\pi/2$, constant;
f_2, $1/u_1$, constant [$1/s^{\frac{1}{2}}$];
f_i, $k/\rho_1 c d_0 (\pi a)^{\frac{1}{2}}$, constant [$1/s^{\frac{1}{2}}$];
F, $(k\rho c)^{\frac{1}{2}}$ [$J/s^{\frac{1}{2}}m$ degC];
g, gravitational acceleration [m/s^2];
G, vaporized mass fraction for individual bubble, or mass ratio of vapour in bubble and corresponding region of influence on relaxation microlayer;
G^*, $(C_{1,m}/C_{1,p})G$ = vaporized mass fraction for individual bubble in binary mixture, or mass ratio of bubble in mixture and corresponding region of influence on relaxation microlayer in pure less volatile component, $G^* = G$ in pure liquids;
G', $= (A_i/A_w)G$, vaporized mass fraction for one active nucleus with respect to entire area A_w of heating surface;
G'', $= mG'$, vaporized mass fraction for all active nuclei with respect to entire area A_w of heating surface, $G''_{max} = G_{max}$;
Gr, Grashof number;
h, coefficient of heat transfer [W/m^2 degC];
h^*, $= k/(\pi at)^{\frac{1}{2}}$, coefficient of heat transfer for conduction with sudden change in surface temperature [W/m^2 degC];
H, $= 2BR^*$, height of spherical bubble segment [m];
H^*, height of thermal layer at part of bubble boundary, $H^* = 2b^*R^*$ for spherical segment, $H^* = 2bR$ for a sphere [m];
ΔH, $= (4\pi/3)\rho_2 l(R_1^3 - R^3)$ = instantaneous excess enthalpy of removed part of relaxation microlayer during bubble growth at heating surface [J];
k, (liquid) thermal conductivity [W/m degC];
K, $= y/x$ = equilibrium constant of more volatile component in binary mixture (ratio of mass fractions);
l, latent heat of vaporization [J/kg];
L_w, length of heating wire [m];
m, dimensionless number of active nuclei generating vapour bubbles on entire area A_w of heating surface;
m/A_w, number of active nuclei on unit area of heating surface, or nuclei density [m^{-2}];
M, mean error;
M_1, molecular weight of more volatile component in binary mixture;
M_2, molecular weight of less volatile component in binary mixture;
n, $= 3$ (for ordinary nuclei), or 7 (for complex nuclei), dimensionless constant in previous bubble growth equation;
Nu, Nusselt number;
Pr, Prandtl number;
q, $= \Phi/A$ = rate of heat flow through unit area, or heat flux density [W/m^2];
r, distance to bubble centre [m];
R, instantaneous radius of spherical vapour bubble, or equivalent radius of sphere with equal volume for a spherical segment and for a rotation ellipsoid (in case of vibrations) [m];
R^*, radius of spherical bubble segment [m];
R_0, equilibrium bubble radius; $R_0 = 2\sigma T/\rho_2 l \vartheta_0$ for bubbles generated at heating surface [m];
R_1, $= R(t_1)$, (equivalent) bubble radius at the instant t_1 of breaking away from heating surface [m];
R_1^*, $= R^*(t_1)$, radius of spherical bubble segment at instant t_1 [m];
Re, Reynolds number;
S, standard deviation;
t, time elapsed since initial bubble

formation during adherence time, or since bubble departure during delay time [s];

t_1, instant at which bubble is breaking away from heating surface, or departure time [s];

t_2, delay, or waiting time between formation of succeeding bubble on same nucleus and bubble departure [s];

T, absolute boiling point, or saturation temperature at ambient pressure [°K];

$T(x)$, absolute boiling temperature of liquid at bubble boundary in binary liquid mixture [°K];

$T(x_0)$, absolute boiling temperature of original liquid in binary mixture [°K];

$T(y)$, absolute dew temperature of saturated vapour in binary mixture, $T(y) = T(x)$ [°K];

ΔT, $= T(y) - T(x_0) = T(x) - T(x_0)$, temperature difference between dew temperature of vapour in bubbles and boiling temperature of original liquid in binary mixture, or increase in temperature of liquid at bubble boundary with respect to original liquid; $\Delta T = 0$ for pure liquids and for azeotropic mixture [degC];

u, $= t^{\frac{1}{2}}$; $u_1 = t_1^{\frac{1}{2}}$; $u_2 = t_2^{\frac{1}{2}}$ [s$^{\frac{1}{2}}$];

v, propagation velocity of capillary waves [m/s];

V, $= 4\pi b R^2 d$ = volume of relaxation microlayer [m^3];

V_b, $= (\pi/3)\, H^2(3R^* - H) = (4\pi/3)\, B^2(3 - 2B)(R^*)^3$, volume of spherical bubble segment [m^3];

W, $= (4\pi/3)\,\sigma R_0^2 = (16\pi/3)\,\sigma^3(T/\rho_2 l \vartheta_0)^2$, energy required for creation of equilibrium bubble [J];

x, $= x_0/\{1 + (K - 1)G_d\}$, mass fraction of more volatile component in liquid at bubble boundary in binary mixture;

x_0, mass fraction of more volatile component in original liquid in binary mixture;

y, mass fraction of more volatile component in vapour of binary mixture;

z, $= (\frac{1}{2})D_w + (2B - 1)R_1^*$, cylinder radius of maximal intersection with vapour bubbles [m].

Greek letters

α, $=$ arc cos $(2B - 1)$, contact angle characterizing the wetting of the heating surface;

β, $= R/2(at)^{\frac{1}{2}} = C_2/2a^{\frac{1}{2}}$, dimensionless bubble growth coefficient;

γ, $= b^*/B$, dimensionless constant;

δ, thickness of diffusion microlayer in binary mixture [μ or m];

ε, $= 1 - (\rho_2/\rho_1)$, dimensionless constant, which establishes effect of radial convection on bubble growth for small liquid superheatings;

ϑ, instantaneous uniform superheating of relaxation microlayer [degC];

ϑ_0, superheating of heating surface, or initial maximum superheating of relaxation microlayer surrounding part of bubble boundary [degC];

ϑ_1, superheating of heating surface at transition between convection and nucleate boiling [degC];

ϑ^*, $= \vartheta - (\vartheta_0/e)$ [degC];

ϑ_0^*, superheating of contact surface between two semi-infinite bodies [degC];

$\Delta\vartheta_0$, uniform superheating of bulk liquid, [degC];

λ, wavelength of capillary waves at Leidenfrost-point [m];

μ, $= (a/D)^{\frac{1}{2}}$, dimensionless constant relating heat conduction and mass diffusion;

ν, $= 1/(t_1 + t_2)$, frequency of bubble formation on nucleus [1/s];

ξ, $= (2/u_1)u$, dimensionless integration variable;

ρ, density [kg/m^3];
ρ_1, liquid density [kg/m^3];
ρ_2, saturated vapour density [kg/m^3];
σ, surface tension constant [kg/s^2];
τ, $= \rho_1 c\overline{d}/h_w$, relaxation time, or time constant [s];
$\varphi(\varepsilon, \beta)$, $= (\rho_1 c/\rho_2 l)(\vartheta_0 - \Delta T)$, dimensionless bubble growth function according to Scriven's theory for binary liquid mixtures; $\varphi \to 2\beta^2 = C_2^2/2a$ for $\beta \to 0$ (i.e. bubble growth at very small superheatings is increased due to radial convection for $\varepsilon \approx 1$); $\varphi \to (\pi/3)^{\frac{1}{2}}\beta = (\pi/12)^{\frac{1}{2}}(C_2/a^{\frac{1}{2}})$ for relatively large β (i.e. for moderate superheatings);
$\varphi(\varepsilon, \mu\beta)$, $= \rho_1(x_0 - x)/\rho_2)y - x) = (\rho_1/\rho_2)G_d$, dimensionless diffusion function according to Scriven's theory for binary mixtures;
Φ, = rate of heat flow [W].

Subscripts

b, value for individual bubble (mostly omitted), or (for heat flux density) applying to direct vapour formation at heating surface;
bi, (for heat flux density) bubble-induced contribution, or difference between total heat flux and convection contribution, $q_{w,bi} = q_w - q_{w,co}$, $q_{w,b} < q_{w,bi}$ in mixture, $q_{w,b} = q_{w,bi}$ in pure less volatile component;
c, value for complex nuclei in binary mixture;
co, (for heat-flux density) convection contribution;
d, value for mass diffusion;
e, experimental value;
h, value for heat diffusion;
i, applying to region of influence of individual bubble;
m, value in binary mixture;
M, value for mole fractions;
max, value for peak flux conditions;
0, maximum value (exception, R_0);
p, value in less volatile pure component;
t, theoretical value;
w, value for heating surface.

Numerical values for water at atmospheric boiling point

a $= 16{\cdot}9 \times 10^{-8}$ m^2/s;
c $= 4216$ J/kg degC;
D $= 9{\cdot}9 \times 10^{-10}$ m^2/s for 1-butanol in water at 97°C;
g $= 9{\cdot}81$ m/s^2;
k $= 0{\cdot}6825$ W/m degC;
l $= 22{\cdot}56 \times 10^5$ J/kg;
R_0 $= 3{\cdot}3 \times 10^{-5}/\vartheta_0$ m;
β $= 1220\, C_2$;
ε $= 0{\cdot}9994$;
μ, $= 13{\cdot}1$ for 1-butanol in water at 97°C;
ρ_1 $= 958{\cdot}4$ kg/m^3;
ρ_2 $= 0{\cdot}598$ kg/m^3;
$\rho_2 l/\rho_1 c$ $= 0{\cdot}3334$ degC;
σ $= 0{\cdot}0587$ kg/s^2.

1. THE PRESENT KNOWLEDGE OF NUCLEATE BOILING

1.1 *Boiling curves*

HEAT FLUX DENSITY q_w as a function of the temperature difference ("superheating") ϑ_0 between a heating surface and the bulk of a boiling liquid, is commonly called a "boiling curve". A boiling curve consists of a region of natural (or free) convection and a region of nucleate boiling, which occur at moderate superheatings. The number of active sites ("nuclei"), generating vapour bubbles in the region of nucleate boiling increases with increasing superheating (Fig. 1).

Vapour bubbles coalesce frequently in the neighbourhood of the heating surface, if the superheating exceeds a critical value (generally 10–50 degC). The heating surface is then covered with a more or less coherent layer of vapour ("Leidenfrost-phenomenon"). This results in a thermal insulation; the heat flux decreases ("transition boiling"), causing the temperature to increase.

At higher temperatures the heat flux density will again increase with increasing temperature partly due to the contribution of radiant flux. Often, however, burnout at the melting point of the heating material is reached before a stationary state is obtained in the region of "film boiling".

1.2 *The peak flux*

The study of the maximum heat flux density in nucleate boiling ("peak flux") occurring in a pure liquid is very important for practical utilizations. A large number of investigations have been carried out with the purpose to increase the peak flux. A favourable effect occurs due to intensive liquid agitation (Pramuk and Westwater [1, 70]), subcooling of the bulk liquid (Nukiyama [2] and van Wijk and van Stralen [3–5]), preferably in combination with the application of forced convection in linear flow (Schweppe and Foust [6], McAdams *et al.* [7, 8], Kreith and Summerfield [9] and Gunther [10]), vortex flow (Gambill and Greene [11]), application of an electrostatic field (Senftleben [12], Bonjour, Verdier and Weil [13]), use of an oxidized heating surface (Farber and Scorah [14], van Stralen [15] and Averin [16]), and increase of pressure up to one-third of the critical pressure (Cichelli and Bonilla [17] for organic liquids, and Addoms [18], van Stralen [15, 19] and Kazakova [20] for water). The design of most of these experiments is empirical resulting in correlations of dimensionless groups of thermal and flow quantities predicting the effect only of the special parameter investigated. Some of these correlations for the region of nucleate boiling are an extension of the well-known convection equations $Nu(Gr, Pr)$ for free convection or $Nu(Pr, Re)$ for forced convection, eventually (more successful) with the characteristic length taken as the bubble diameter at departure and the characteristic velocity as the initial bubble growth rate.

The observed increase of the peak flux is in general mainly due to an appreciable reduction of the direct vapour formation in the neighbourhood of the heating surface, whence the onset of film boiling is delayed. This underlies also the occurrence of a maximum peak flux at a certain (low) concentration of the more volatile component in binary (or ternary) liquid mixtures boiling at various pressures, up to the critical [21–24, 15, 19, 25, 5]. For instance, in water–methylethylketone boiling at atmospheric pressure, an extremely high maximum occurs at 4·1 wt. % methylethylketone, which amounts to 2·5 times the peak flux in pure water (Fig. 1).

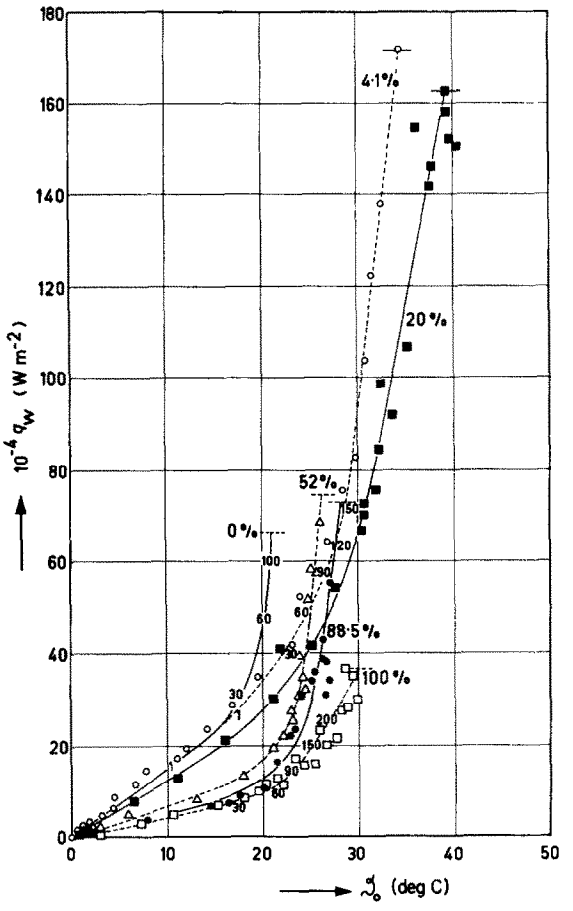

FIG. 1. *Water–methylethylketone.* Boiling curves for convection and nucleate boiling to water and to 4·1 (○), 20 (■), 52 (△), 88·5 (●) and 100 (□) wt. % methylethylketone, all at atmospheric pressure.
Figures by curves for 0, 4·1 and 100% methylethylketone denote number of active nuclei generating vapour bubbles on 1 cm^2 of a horizontal platinum heating surface.

Increased peak fluxes in subcooled binary mixtures were investigated by van Stralen [4, 5], for free convection and by Carne [26] for forced convection.

1.3 *Recent trends*

Recently, new information on nucleate boiling has become available from a number of valuable fundamental contributions, some of which will be discussed more extensively below:

(i) Growth rates of free vapour bubbles in uniformly superheated liquids could be treated theoretically (Forster and Zuber [27] and Plesset and Zwick [28]), even for the rather complex case of binary liquid mixtures (van Wijk, Vos and van Stralen [22], Bruijn [29] and Scriven [30]). Van Stralen [31] showed that the occurrence of a slowing down of bubble growth at the same low concentration of the more volatile component, at which the maximum peak flux has been observed previously, and which had been predicted by van Wijk, Vos and van Stralen [22], is in good agreement with Scriven's theory.

The growth rate of a bubble in a pure component is not a hydrodynamic problem but depends only on the heat flow towards the bubble boundary to satisfy the heat requirement of evaporation. In mixtures, heat diffusion is linked with mass diffusion of the more volatile component, as this component is rapidly exhausted in the liquid near the bubble. In addition, Scriven [30] established the effect of radial convection resulting from unequal phase densities, by which bubble growth rates at small liquid superheatings are increased considerably.

(ii) Experimental investigations on the growth rate of free or released bubbles using high speed photography on pure liquids (Jakob [32, 33], Dergarabedian [34] and van Wijk and van Stralen [35] on water and Wanninger [36] on propane at high pressures) and on binary mixtures (Benjamin and Westwater [38, 71] on water–ethyleneglycol, van Wijk and van Stralen [35] on water–methylethylketone and van Stralen [39] on water–1-butanol) were in good agreement with theory. The reader is referred to Section 1.5 and to the literature for a chronological survey, for a description of the experimental setup and for details concerning the photographic technique [35, 39, 4, 31].

(iii) Temperature fluctuations in coincidence with periodic initial bubble formation have been observed at the contact area between the heating surface and the adhering thermal liquid boundary layer. Different interpretations of this phenomenon have created much controversy about the understanding of the mechanism of nucleate boiling, cf. Section 1.4.

(iv) Hsu and Graham [40, 41] (cf. also Leppert and Pitts [42]), Béhar and Séméria [43] and Brauer [44] made observations of the thermal boundary layer adhering to the heating surface in water from (colour) schlieren photographs. An initially rapidly growing vapour bubble at the wall removed this thermal microlayer locally away from the surface.

(v) The extremely important results of (iv) are in fair agreement with the new theory presented here (Section 1.6), which was deduced originally from high-speed motion pictures on bubble growth: the excess enthalpy of the thermal microlayer, which is pushed away from the surface by the growing bubble, is entirely used to supply latent heat for direct vaporization in pure liquids, but only partly so in binary mixtures.

1.4 *Temperature fluctuations*

Sudden dips of the local temperature occur

periodically at the area of contact between the heating surface and a boiling liquid, both in the regions of nucleate boiling and film boiling. Observations could be made by using a special thermocouple device with low response time, according to Bendersky [45]. Moore and Mesler [46] studied this effect in water (nucleate boiling), Madsen and Bonilla [47] in liquid metals (nucleate boiling), Rogers and Mesler [48] in water (nucleate boiling), Madsen [49] in water (both nucleate boiling and film boiling), and Bonnet, Macke and Morin [50] in water (nucleate boiling). The onset instant of the rapid temperature drop is shown to coincide with the high initial growth rate of a vapour bubble, which is generated on the nearest active nucleus at the heating surface, according to Bonnet, Macke and Morin [50] and to Rogers and Mesler [48] using a synchronization device of both phenomena. The local temperature increases to the original superheating shortly before bubble departure and during the delay time, until the succeeding bubble is generated on the same nucleus. The shape of the temperature vs. time curves may sometimes be more complex since response is given then to fluctuations due to a superposition of bubbles which are growing simultaneously on various neighbouring nuclei.

The interpretation of the observed temperature fluctuations, which is highly important for the understanding of the mechanism of nucleate boiling and possibly also for the explanation of material fatigue in boiling, is rather difficult. Moore and Mesler [46] stated the hypothesis, that a very thin (order of magnitude of 1 μ) liquid microlayer between a vapour bubble and the heating surface exists and evaporates rapidly, thus being responsible for the calculated very high heat flux densities during initial bubble growth. Contrarily, Madsen [49] assumed the existence of a considerably thicker liquid microlayer with uniform temperature at the bottom of the bubble, which is heated periodically during the delay time and is cooled during bubble growth. Consequently, much lower local heat flux densities are predicted, and the heat transfer mechanism breaks up in two stages: (i) heat exchange between surface and cooled microlayer, and (ii) exchange of excess enthalpy between superheated microlayer and growing vapour bubble. The thickness of Madsen's "relaxation" microlayer is expected to be approximately 25 μ, i.e. $1/c\vartheta_0$ times the thickness of Moore and Mesler's "evaporation" microlayer, in good agreement with Madsen's values, cf. Section 3.19.

In the "delay time" (or "waiting period" between departure of the bubble and initial formation of the succeeding bubble on the same active site) colder liquid of the bulk (slightly superheated above saturation temperature) is replacing the original highly superheated thermal boundary layer at the heating surface.

Stephan [51, 52] and Kast [53] describe the heat transmission from the surface during the delay time. Stephan is using Pohlhausen's equation [54] which, however, gives inaccurate values as the direction of the liquid flow is uncertain. Most other workers (Han [55], cf. also Rohsenow [56], and Bonnet, Macke and Morin [50]) make use of the transient conduction equation for a semi-infinite body, whence the heat flux density at the surface is given by:

$$q_w = f_1 \frac{k\vartheta_0}{(\pi a t)^{\frac{1}{2}}} = \frac{f_1}{\pi} \frac{(\pi k \rho c)^{\frac{1}{2}}}{t^{\frac{1}{2}}} \vartheta_0 \qquad (1)$$

We shall show, that the factor $f_1 = 1$ for constant temperature (a step change in temperature at the wall), which is allowed for short periods only, according to Hudson and Bankoff [57]. Viz., the semi-infinite liquid and heating bodies (with initial uniform temperature T and $T + \vartheta_0$ respectively) are assumed to come into contact at the instant $t = 0$. The superheating of the contact surface approximates a constant value ϑ_0^*:

$$\vartheta_0^* = \frac{F_w}{F_w + F} \vartheta_0$$

and

$$q_w = \frac{F}{(\pi t)^{\frac{1}{2}}} \vartheta_0^* = \frac{F_w}{F_w + F} \frac{F}{(\pi t)^{\frac{1}{2}}} \vartheta_0,$$

where $F = (k\rho c)^{\frac{1}{2}}$ and $F_w = (k_w\rho_w c_w)^{\frac{1}{2}}$ refer to the liquid and to the heating material, respectively. These equations are for $F \ll F_w$, which case applies here, simplified to:

$$\vartheta_0^* = \vartheta_0$$

and

$$q_w = \frac{F}{(\pi t)^{\frac{1}{2}}}\vartheta_0,$$

i.e. equation (1) with $f_1 = 1$.

The factor $f_1 = \pi/2$ for constant heat flux density at the wall (sudden start of heating at $t = 0$, cf. Carslaw and Jaeger [58]). The different results of the calculations by the various workers is principally based on the interpretation of the meaning of the thermal quantities k and $a = k/\rho c$ in equation (1). Moore and Mesler [46] and Bonnet, Macke and Morin [50] take $k_w/a_w^{\frac{1}{2}}$, i.e. the value for the semi-infinite heating body (stainless steel), thus obtaining very high constant local heat flux values from the surface during bubble growth at the wall; contrarily, Han [55] (cf. also Rohsenow [56]) lets this quantity refer to the semi-infinite bulk liquid, whence much smaller local heat flux densities are obtained.

We shall show here that the last statement is correct, assuming pure conduction, thus neglecting convection on account of the short duration (approximately 1–10 ms) of the temperature dips. For stainless steel (all data are given at a temperature of 100°C):

$$k_w = 16{\cdot}8 \text{ W/m degC},$$
$$\rho_w = 7{\cdot}9 \times 10^3 \text{ kg/m}^3,$$

and

$$c_w = 503 \text{ J/kg degC},$$

whence

$$(\pi k_w\rho_w c_w)^{\frac{1}{2}} = 1{\cdot}45 \times 10^4 \text{ J/s}^{\frac{1}{2}}\text{m}^2 \text{ degC};$$

for platinum:

$$k_w = 71{\cdot}2 \text{ W/m degC},$$
$$\rho_w = 21{\cdot}4 \times 10^3 \text{ kg/m}^3,$$

and

$$c_w = 138 \text{ J/kg degC},$$

whence

$$(\pi k_w\rho_w c_w)^{\frac{1}{2}} = 2{\cdot}56 \times 10^4 \text{ J/s}^{\frac{1}{2}}\text{m}^2 \text{ degC};$$

for copper

$$k_w = 381 \text{ W/m degC},$$
$$\rho_w = 8{\cdot}8 \times 10^3 \text{ kg/m}^3,$$

and

$$c_w = 377 \text{ J/kg degC},$$

whence

$$(\pi k_w\rho_w c_w)^{\frac{1}{2}} = 6{\cdot}45 \times 10^4 \text{ J/s}^{\frac{1}{2}}\text{m}^2 \text{ degC};$$

for water

$$k = 0{\cdot}683 \text{ W/m degC},$$
$$\rho = 958 \text{ kg/m}^3,$$

and

$$c = 4216 \text{ J/kg degC},$$

whence

$$(\pi k\rho c)^{\frac{1}{2}} = 0{\cdot}297 \times 10^4 \text{ J/s}^{\frac{1}{2}}\text{m}^2 \text{ degC},$$

a considerably smaller value, whence the condition $F \ll F_w$ is satisfied here.

A maximum temperature dip of 15 degC, e.g. which is reached in 10 ms, corresponds to constant heat flux density at the surface of $10{\cdot}9 \times 10^5$ W/m^2 (stainless steel), $19{\cdot}3 \times 10^5$ W/m^2 (platinum), $49{\cdot}4 \times 10^5$ W/m^2 (copper) and $2{\cdot}23 \times 10^5$ W/m^2 (water). The temperature dip at the surface of contact between two touching semi-infinite bodies 1 and 2 of originally different uniform temperatures is, in the absence of heat sources, inversely proportional to $\{(k\rho c)_1/(k\rho c)_2\}^{\frac{1}{2}}$, on account of continuity of the heat flux density at the contact surface.

Consequently, for steam bubbles generated on a copper surface with a superheating $\vartheta_0 = 15{\cdot}7$ degC, the ratio of the corresponding temperature dips at the surface in the water and the copper amounts to $6{\cdot}45/0{\cdot}297 = 21{\cdot}7$. If the actually measured temperature dip of 15·0 degC

should refer to the copper, a corresponding dip of 325 degC must occur in the water. This is impossible as this value cannot exceed ϑ_0. It follows, that the measured temperature dip refers mainly to the temperature of the body with lowest contact coefficient kpc, i.e. the liquid here. The same result has been obtained experimentally by Madsen [49]. Maximum temperature dips in copper and stainless steel with boiling water should be in the ratio 1·45/6·45 = 0·225. Actually no perceptible differences between the maximum dips occurred when the copper heating plate was substituted for the stainless steel plate.

The problem discussed here is highly important for the determination of the fraction of the total heat flux density which is transferred directly to the bubbles during adherence to the heating wall (or the ratio of the direct vapour formation to the total vapour formation). The estimates for water vary from a fraction of the order of magnitude of 10^{-2} to 10^{-1} (Jakob [32, 33]), to 0·80 at peak flux conditions (Rallis and Jawurek [59]), and even to 1·00 (Bonnet, Macke and Morin [50]. The latter estimate must be incorrect, however, as a subsequent growth of released vapour bubbles is occurring during their rise through the slightly superheated bulk liquid (Jakob [32, 33], van Wijk and van Stralen [35] and van Stralen [39]).

1.5 *Bubble growth in binary mixtures*

The study of binary liquid mixtures has several advantages over pure liquids as the direct vapour formation at the heating surface can be reduced appreciably due to a slowing down of bubble growth and corresponding decreased departure size. As a consequence, higher nucleate boiling peak flux densities occur at a certain (low) concentration of the more volatile component, which can be derived from equilibrium data [22, 24, 25, 15, 19, 60, 4, 5, 31], cf. Fig. 2 for the system water–1-butanol.

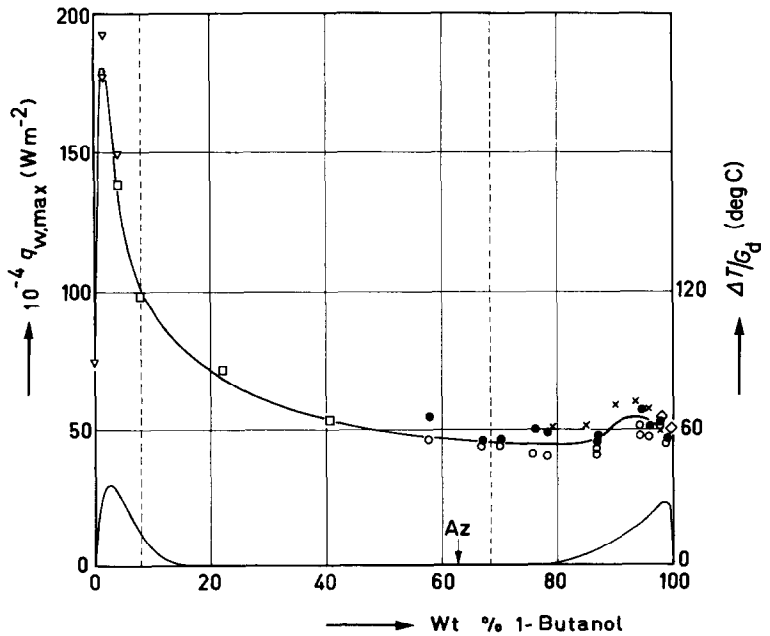

FIG. 2. *Water–1-butanol.* Peak flux as a function of composition at atmospheric pressure. Measurements carried out with same platinum heating wire are represented by same figures. Az = azeotrope. Dotted vertical lines indicate boundaries of region of demixing at azeotropic boiling point. Bottom curves represent $\Delta T/G_d$, cf. Part II.

In addition, the study of mixtures is advantageous for a second reason: the region of isolated bubbles (cf. Gaertner [61] and Zuber [62]) in "positive" mixtures—in which the more volatile component has the lowest surface tension—is extended nearly to peak flux conditions on account of a diminished tendency for bubble coalescence due to the Marangoni-effect (Hovestreijdt [63]). Hence, experimental data on bubble growth, which are obtained at moderate nucleate boiling heat fluxes are also representative for higher values.

1.6 *A new theory of nucleate boiling*

The growth rate of released, free vapour bubbles has been studied previously, both experimentally and theoretically. Initial growth rates of bubbles generated at a nucleus on a heating surface are investigated in the present work. As a consequence, the author's modification of the theories by van Wijk, Vos and van Stralen [22], Scriven [30] and Bruijn [29], for bubble growth in binary mixtures (including pure liquids, evidently) is extended to the more complex case of time-dependent liquid superheating. This theory is leading to a new approach of the mechanism of nucleate boiling by considering periodic bubble generation as a relaxation phenomenon of the superheating of the thermal boundary layer at the heating surface. This thin liquid layer is pushed away locally (due to the radial motion of the bubble boundary) from the heating surface during rapid initial bubble growth and is surrounding a part of the boundary bubble until departure from the surface. Colder liquid at saturation temperature is flowing to the nucleus and heated during the delay time before formation of the succeeding bubble.

At first, it was believed that the heat supply to a growing bubble at a heating surface originated only from the thin thermal microlayer at the base. However, this conception resulted in discrepancies from experimental growth data. The next approach proved to be correct; heat inflow was assumed to occur through a spherical segment with height $H^* = 2b^*R^*$ of the bubble boundary. The bubble is assumed to be a spherical segment, the height H of which was also taken as being proportional to the instantaneous bubble radius: $H = 2BR^*$, i.e. the ratio of the effective part of the boundary to the whole bubble area was taken as constant during entire bubble growth at the heating surface, up to the instant of departure. The value of the constant "wetting parameter" is shown to be $B = 0{\cdot}75$, which is attributed to the imperfect wetting of the heating surface by the liquid. The angle of contact $\alpha = \pi/3$ corresponding with this value of B could be calculated from

$$\cos\alpha = \frac{2BR^* - R^*}{R^*} = 2B - 1 \qquad (2)$$

and is in good agreement with the experimental value.

Afterwards, this mechanism—which was suggested by making a comparison of the author's originally incomplete theory [31, 4] and experimental bubble growth [35, 39, 60, 31]—proved to be in good agreement with recent shadowgraph studies by Béhar and Séméria [43] and by Brauer [44]. Béhar and Séméria made observations of the removed hot boundary layer from high-speed schlieren motion pictures.

Brauer [44] deduced large temperature gradients from colour schlieren photographs in the liquid adjacent to vapour bubbles, which were generated at a vertical heating rod. The deflected light rays were incident upon narrow coloured glass strips. The colour of the transmitted glass strip is a measure for the angle of deflection and hence also for the relative temperature gradient. Grigull [68] found, when boiling water on a heated mercury surface, that a thin mercury skin is originally ascending with the bubbles, before descending under gravity.

It may be noticed here, that both the effects of wetting (due to interfacial tension resulting in a fixed angle of contact), and nucleation properties of the heating material are included in the theory. The well-known independence (Averin

[16], van Stralen [15] and Rallis and Jawurek [59]) of the peak flux from the shape of the nucleate boiling part of the boiling curve, which is determined by the nucleation function, is also obvious now.

1.7 *Advantages over previous treatments*

Previous suggestions of the mechanism of nucleate boiling, e.g. the semi-empirical correlations proposed by Jakob [32, 33], Rohsenow [64], Kutateladze [65] and Zuber and Tribus [66, 67] predicted lower nucleate boiling peak flux values in binary mixtures in comparison to the pure less volatile component, thus being principally incorrect. Contrarily, the peak fluxes predicted by the new theory are in quantitative agreement with experimental data. Hence, both nucleate boiling peak flux densities, and the composition of the binary mixture at which the maximum peak flux occurs, can be calculated now.

The differences and similarities of the present theory with Madsen's [49] and Han's [55] approach for pure liquids are obvious. Also, the author cannot agree with Madsen's interpretation of the large temperature dips (up to 75 degC in water) observed during stable film boiling, which he suggests to be caused by droplets, or filaments torn from the stable liquid surface, breaking through the protecting vapour film and touching the thermocouple. This conclusion is disproved by high speed motion pictures taken by Westwater and Santangelo [69, 70] on boiling methanol, and by van Stralen [72] on ethanol. The fluctuations must be due to the relatively large thermal diffusivity of the thin vapour film, through which a sudden temperature jump is travelling nearly undamped.

Han [55] (cf. also Rohsenow [56]) made no distinction between the equivalent liquid thermal conduction layer $d_w = 2(1 - 1/e)d_0 = 4(3/\pi)^{\frac{1}{2}}(1 - 1/e)(at_1)^{\frac{1}{2}} = (4/\pi)(1 - 1/e)(\pi at_2)^{\frac{1}{2}}$, c.f. Part II, at the heating surface, and the thickness $d_b = (\pi/3)^{\frac{1}{2}}(at_1)^{\frac{1}{2}}$ of the equivalent conduction layer surrounding a "free" vapour bubble in a pure liquid at the instant of departure. Moreover, the heat flow must then in both layers be directed to the liquid, which applies only to condensation and not to growth of bubbles.

1.8 *The present investigations*

At present, initial growth rates of vapour bubbles generated on horizontal platinum heating wires are studied both theoretically and experimentally in water, in 4·1 wt. % methylethylketone in water, and in 1·5 % and 6·0 wt. % 1-butanol in water, all boiling under atmospheric pressure. In addition, both the bubble delay time, frequency and departure size, and the mass fraction vaporized at the heating surface, are investigated resulting in an expression for the peak flux density.

In the near future, the dependence of the peak flux on initial rapid bubble growth and subsequent condensation rates in "surface" (or "local") boiling to subcooled mixtures, will be studied. Higher condensation rates in mixtures are predicted and compared with results of Volmer and Flood [73–75] and Froemke, Bloomquist and Anderson [76] on condensation of supersaturated water–ethanol and water–methanol vapour mixtures, respectively. Moreover, the effect of pressure on peak flux will be discussed separately.

2. GROWTH OF VAPOUR BUBBLES AT CONSTANT LIQUID SUPERHEATING

2.1 *Introduction*

The growth rate of a vapour bubble, which is generated at a superheated heating surface can be derived theoretically on the following assumptions:

(1) For convenience, we assume the bubble to be surrounded by a thin boundary layer with thickness d_b, through which heat is transmitted by conduction only, i.e. the temperature gradient must have the same value throughout the layer. Strictly speaking, however, this is not necessary, but only the weaker condition that the temperature gradient at the bubble boundary equals ϑ_0/d_b, has to be satisfied.

(2) The dew temperature, denoted by T, of the saturated vapour in the bubble space is uniform due to the large thermal diffusivity of the vapour, independent of time.
(3) The initial (liquid and surface) temperature in the neighbourhood of the generating nucleus is denoted by $T + \vartheta_0$, i.e. the superheating is ϑ_0.
(4) The heating surface is initially covered with a conduction layer with thickness $d_w = k/h_w = k\vartheta_0/q_w$, in which the initial temperature at zero time decreases linearly from $T + \vartheta_0$ at the heating surface to $T + \Delta\vartheta_0$.
(5) The small superheating of the bulk liquid $\Delta\vartheta_0$ is constant outside the boundary layer at the heating surface.
(6) The radius R of the (spherically symmetric) growing bubble in a superheated liquid of uniform superheating ϑ_0 is given as a function of time t by the expression:

$$R = C_1\vartheta_0 t^{\frac{1}{2}}$$

where C_1 is called the growth constant in accordance with Plesset and Zwick [28, 31], Forster and Zuber [27, 31], and Scriven [30, 31].
(7) The growth of the bubble is due to the simultaneous cooling of an adjacent superheated liquid microlayer surrounding a part of the bubble boundary. This microlayer has a uniform temperature $T + \vartheta$, where $0 \leqslant \vartheta \leqslant \vartheta_0$, with the initial condition: $\vartheta = \vartheta_0$ for $t = 0$; the thickness of the layer is denoted by $d(t)$.

The assumptions (1), (2) and (6) are in agreement with the theories by Bošnjaković [77], Forster and Zuber [27], Plesset and Zwick [28], Bruijn [29] and Scriven [30] and with experimental results by Prüger [78], Dergarabedian [34] and van Stralen [31, 4], the assumption (5) agrees with experimental results by Jakob [32, 33], assumption (7) refers to Section 3; it will be shown there that the temperature of the adjacent liquid microlayer decreases rapidly during the time t_1 of adherence of the bubble to the heating surface, and increases gradually during a delay time t_2 after which the succeeding bubble is generated on the same nucleus. This result is in agreement with the periodic temperature fluctuations at the heating surface which have been observed by Moore and Mesler [46] and other workers.

2.2 *Free bubbles*

2.2.1 *Pure liquids.* The radius R of a free, spherically symmetric growing vapour bubble, the boundary of which is entirely surrounded by an infinite volume of superheated liquid with a uniform superheating ϑ_0 can be derived from the heat flux density equation:

$$\frac{\Phi}{A_1} = k\left(\frac{\partial\vartheta}{\partial r}\right)_{r=R} = k\frac{\vartheta_0}{d_b} = \rho_2 l\frac{\mathrm{d}R}{\mathrm{d}t}, \qquad (3)$$

where the bubble area:

$$A_1 = 4\pi R^2. \qquad (4)$$

The thickness d_b of the surrounding boundary layer of liquid, through which heat is transmitted towards the bubble by thermal conduction, amounts to [28, 31]:

$$d_b = \left(\frac{\pi}{3}\right)^{\frac{1}{2}}(at)^{\frac{1}{2}} = 2\frac{k}{\rho_2 l C_1}t^{\frac{1}{2}} = 2\frac{k}{\rho_2 l C_1}u, \qquad (5)$$

where for abbreviation:

$$u = t^{\frac{1}{2}}. \qquad (6)$$

The thermal diffusivity of the liquid

$$a = \frac{k}{\rho_1 c}. \qquad (7)$$

By substitution of (5) in (3) it follows:

$$\frac{\mathrm{d}R}{\mathrm{d}t} = \frac{k}{\rho_2 l}\frac{\vartheta_0}{d_b} = \left(\frac{3}{\pi}\right)^{\frac{1}{2}}\frac{k}{\rho_2 l a^{\frac{1}{2}}u}, \qquad (8)$$

whence the bubble radius is expressed by the growth equation:

$$R = \left(\frac{12}{\pi}\right)^{\frac{1}{2}}\frac{(k\rho_1 c)^{\frac{1}{2}}}{\rho_2 l}\vartheta_0 t^{\frac{1}{2}} = \left(\frac{12}{\pi}\right)^{\frac{1}{2}}\frac{k}{\rho_2 l a^{\frac{1}{2}}}\vartheta_0 t^{\frac{1}{2}} = C_1\vartheta_0 u = C_2 u, \qquad (9)$$

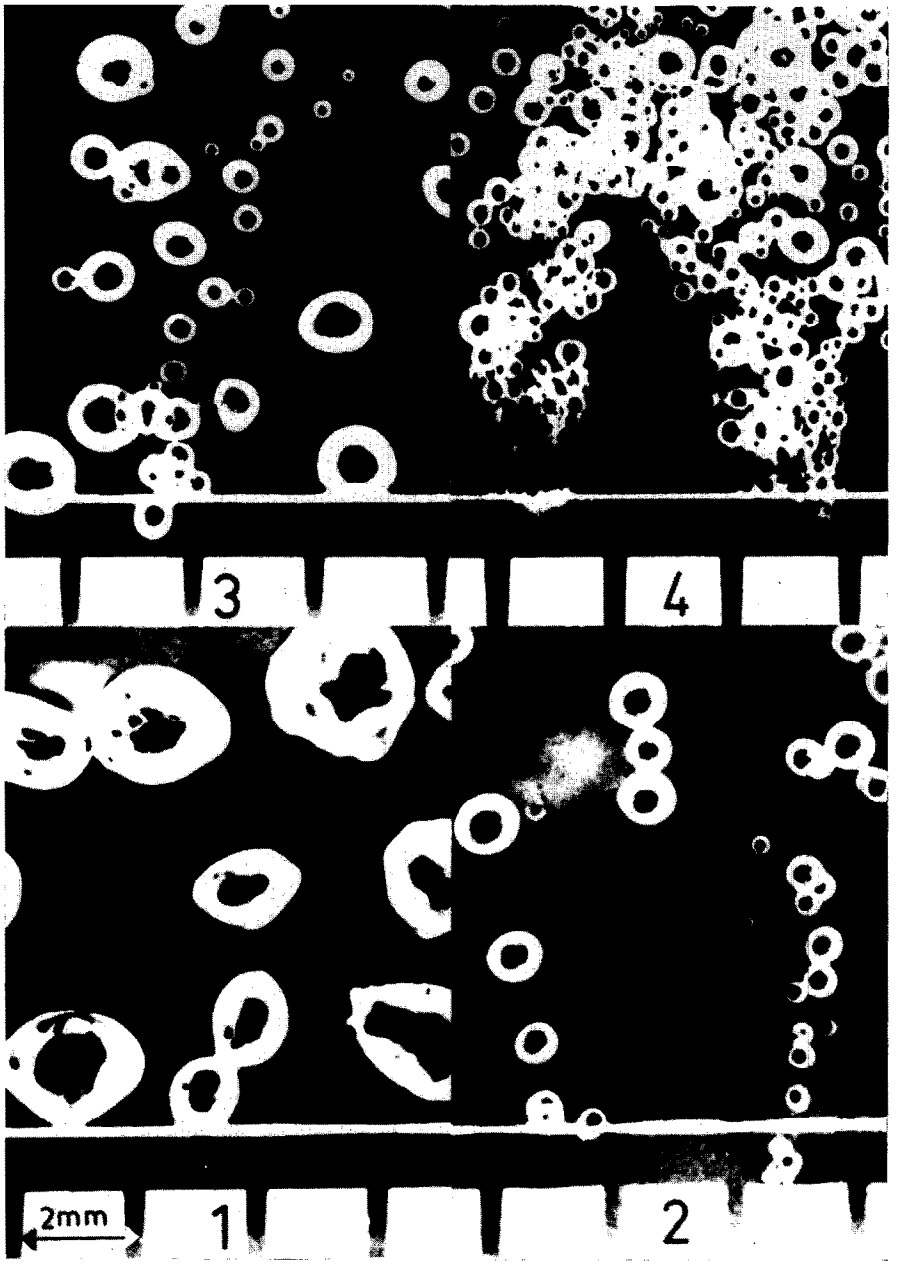

FIG. 3. *Water–methylethylketone and water–1-butanol.* Photographs, showing slowing down of bubble growth and decreased bubble size at instant of breaking away from 200 μ-diameter platinum heating wire, in 4·1 wt. % methylethylketone (2), and in 1·5% (3) and 6·0 wt. % 1-butanol (4) in comparison to water (1). Heat flux density in nucleate boiling $q_w = 45 \times 10^4$ W/m².

Bubble clusters occur on complex nuclei in 6·0% 1-butanol. Bubbles in mixtures leave wire perpendicularly, i.e. sometimes downwards. A 2-mm scale is visible at the bottom of the photographs.

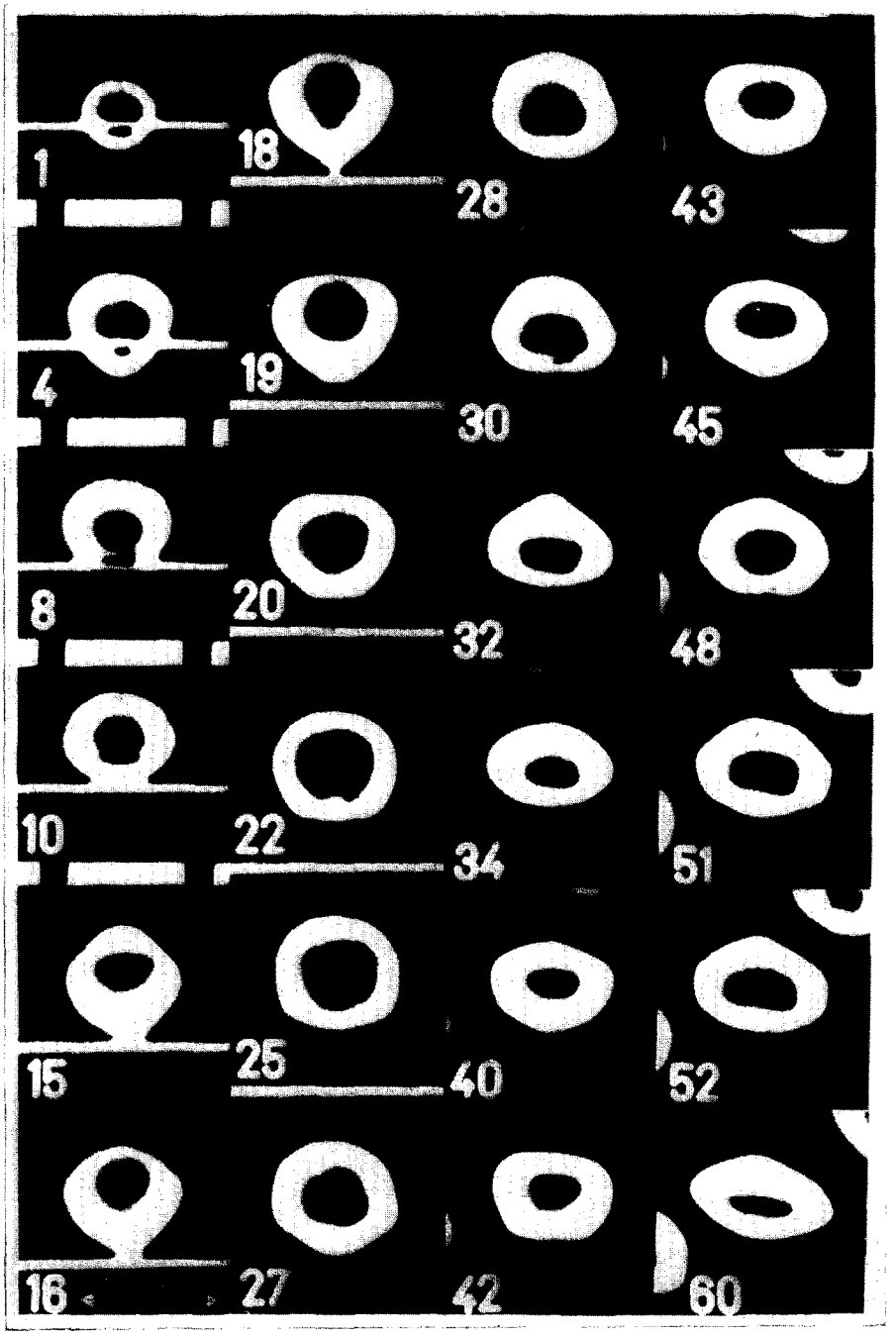

FIG. 4. *1·5 wt. % 1-butanol.* Growth during adherence and subsequent growth after departure of vibrating vapour bubble *a*, cf. Table 1. The bubble is oscillating about the spherical shape. Most important mode of vibration is the slowest, fundamental harmonic, in which a sphere is transformed periodically into a rotation ellipsoid. Higher modes of vibration can also be observed.

Number — number of frame, frequency 3400 frames per second. Frame No. 0 shows no bubble on the nucleus. A 2-mm scale is visible on the bottom of the first four photographs.

Table 1. Data are taken at a constant heat flux density $q_w = 44{\cdot}8 \times 10^4$ W/m²

Liquid	Bubble	$10^4 R_1$ (m)	$10^4 t_1$ (s)	$10^4 t_2$ (s)	$10^4(t_1+t_2)$ (s)	t_2/t_1	ν (1/s)	$10^2 \nu R_1$ (m/s)	$10^5 \nu R_1^2$ (m²/s)	$10^8 \nu R_1^3$ (m³/s)	$10^6(4\pi/3)\rho_2 l R_1^3$ (J)	$10^4(4\pi/3)\rho_2 l \nu R_1^3$ (W)	$10^4(4\pi/3)\rho_2 l \overline{\nu R_1^2}$ (W)	10^{-4} m/A_w (1/m²)	10^{-4} $q_{w,b}$ (W/m²)	10^{-4} q_w (W/m²)	10^{-4} $q_{w,co}$ (W/m²)	10^{-4} $q_{w,bi}$ (W/m²)	$q_{w,b}/q_{w,bi}$
Water																			
$C_1 = 24 \times 10^{-4}$	a†	11·0	76·7	123·3	200·0	1·61	50·0	5·50	6·05	6·65	7537	3768							
m/s‡ degC	e†	10·0	66·7	133·3	200·0	2·00	50·0	5·00	5·00	5·00	5661	2830							
$\vartheta_0 = 20$ degC	b†	11·0	74·8	125·2	200·0	1·67	50·0	5·50	6·05	6·65	7537	3768							
	f	11·9	71·7	128·3	200·0	1·77	50·0	5·95	7·08	8·43	9538	4769							
	g	8·12	46·7	55·0	101·7	1·18	98·4	7·99	6·48	5·27	3031	2981							
	h	8·80			100·0		100·0	8·80	7·74	6·81	3856	3856							
													3664	45	16·5	44·8	29·7	15·1	1·10
4·1% methyl-ethylketone																			
$C_1 = 6 \times 10^{-4}$	a†	4·3	74·8	30·2	105·0	0·40	95·0	4·09	1·76	0·757	435	413							
m/s‡ degC	b†	3·7	65·6	51·1	116·7	0·78	85·7	3·17	1·17	0·433	277	237							
$\vartheta_0 = 24$ degC	f	2·58	43·3	25·0	68·3	0·58	146·3	3·77	0·973	0·251	93·8	1373							
	g	1·95	46·7	11·7	58·3	0·25	171·4	3·34	0·651	0·127	40·5	69							
	h†	1·82	10·0	25·0	35·0	2·50	285·7	5·20	0·946	0·172	33·0	94							
	i†	1·82	8·33	3·33	11·67	0·40	857·1	15·60	2·839	0·517	33·0	282							
	j	0·97	5·00	6·67	11·67	1·33	857·1	8·31	0·806	0·782	5·0	43							
													182	50	0·92	44·8	36·0	8·8	0·10
1·5% 1-butanol																			
$C_1 = 18 \times 10^{-4}$	b†	7·0	48·3	131·7	180·0	2·73	55·5	3·88	2·72	1·90	1909	1059							
m/s‡ degC	c†	7·7	55·0	70·0	125·0	1·27	80·0	6·16	4·76	3·67	2542	2035							
$\vartheta_0 = 21$ degC													1549‡	55	8·5‡	44·8	31·4	13·4	0·65‡

† Succeeding bubbles on some nucleus, cf. also Table 1 of Part I.
‡ Actually considerably smaller due to presence of complex nuclei.

since $R = R_0$ for $t = 0$, a value of the order of 10^{-5}–10^{-6} m, cf. equation (43), which can be neglected.

The coefficient

$$C_1 = \left(\frac{12}{\pi}\right)^{\frac{1}{2}} \frac{(k\rho_1 c)^{\frac{1}{2}}}{\rho_2 l} \tag{10}$$

shall be called the growth constant, since C_1 is independent of ϑ_0, and

$$C_2 = C_1 \vartheta_0 \tag{11}$$

is called the growth factor which determines actual growth rates of bubbles in a boiling vessel.

2.2.2 *Binary mixtures.* The rate of bubble growth in a pure component depends on heat inflow towards the bubble boundary to satisfy the heat requirement of evaporation. In mixtures, the heat diffusion is linked with mass diffusion of the more volatile component. A lower mass diffusivity of the more volatile component results in a decreased bubble growth.

The growth equation (9) is also valid for binary mixtures. However, the growth constant C_1 for a constant liquid superheating depends then on the concentration of the more volatile component according to:

$$C_1 = \left(\frac{12}{\pi}\right)^{\frac{1}{2}} \frac{D^{\frac{1}{2}}}{\frac{\rho_2}{\rho_1}\left\{\left(\frac{D}{a}\right)^{\frac{1}{2}} \frac{l}{c} + \frac{\Delta T}{G_d}\right\}} = \left(\frac{12}{\pi}\right)^{\frac{1}{2}} \frac{a^{\frac{1}{2}}}{\frac{\rho_2}{\rho_1}\left\{\frac{l}{c} + \left(\frac{a}{D}\right)^{\frac{1}{2}} \frac{\Delta T}{G_d}\right\}}, \tag{12}$$

where

$$\frac{\Delta T}{G_d} = -x_0(K-1)\left(\frac{\mathrm{d}T}{\mathrm{d}x}\right)_{x=x_0} \tag{13}$$

It is seen from (12), that C_1 shows a minimum (i.e. bubble growth is slowed down) in coincidence with a maximum in $\Delta T/G_d$, usually occurring at a small concentration of the more volatile component. The concentration of this maximum can be derived from equilibrium data, cf. (13). Equation (10) is a special case of (12), since the increase in dew temperature of saturated vapour, ΔT, is zero in a pure liquid (Fig. 2).

2.2.3 *Comparison with experimental results.* Theoretical bubble growth predicted by equations (9) and (12), respectively, is in quantitative agreement with experimental results (at atmospheric pressure) by Dergarabedian [34] for water at various liquid superheatings; by van Wijk and van Stralen [35, 60, 5] for the binary system water–methylethylketone, cf. Fig. 3, by van Stralen [39, 60, 5] for water–1-butanol, cf. Figs. 3 and 4, and by Benjamin and Westwater [38, 70, 7] for water–ethyleneglycol.

2.3 *Growth for partial heat supply*

2.3.1 *Bubble is a sphere with radius R.* If heat is supplied to the bubble boundary only through a spherical segment of height

$$H^* = 2bR, \tag{14}$$

where b = constant, with $0 < b \leqslant 1$, i.e. through the area

$$A_2 = 2\pi R H^* = 4\pi b R^2 = bA_1.$$

Equation (3) has to be extended to a more general expression for the heat flow:

$$\Phi = A_2 k \frac{\vartheta_0}{d_b} = A_1 \rho_2 l \frac{\mathrm{d}R}{\mathrm{d}t}, \tag{15}$$

whence the right-hand side of the bubble growth equation (9) must be multiplied here by a factor b, which decreases the growth of the bubble:

$$R = bC_1\vartheta_0 u = bC_2 u. \tag{16}$$

2.3.2 *Bubble is a spherical segment with radius R*.* The more general case will now be considered of partial heat supply to the boundary of a spherical bubble segment with height $H = 2BR^*$. Heat is transmitted only through a spherical segment with height $H^* = 2b^*R^*$, where $b^* = \gamma B$ and $\gamma \leqslant 1$ (Fig. 5). The "wetting parameter" B and the "microlayer parameter" b^* are both assumed to be constant. The imperfect wetting of the heating surface is incorporated in the theory. Time-independence of B implies a constant wetting angle and thus geometrically similar bubble growth during adherence to the heating surface.

The required heat for vaporization is supplied by conduction towards a part of the bubble boundary, analogous to equation (15):

$$\rho_2 l \frac{dV_b}{d_b} = 4\pi b^*(R^*)^2 k \frac{\vartheta_0}{d_b}$$

with

$$V_b = (\pi/3)H^2(3R^* - H) = (4\pi/3)B^2(3 - 2B)(R^*)^3,$$

whence:

$$\rho_2 l B^2(3 - 2B)\frac{dR^*}{dt} = b^* k \frac{\vartheta_0}{d_b}$$

A factor $b^*/B^2(3 - 2B) = \gamma/B(3 - 2B)$ is introduced in the right-hand side of (16) instead of b^*. In the special case of heat supply towards the entire boundary of the spherical bubble segment, i.e. $b^* = B$, this factor is reduced to $1/B(3 - 2B)$, in accordance with Donald and Haslam [79].

The equation for the wetting parameter B is:

$$\frac{b^*}{B^2(3 - 2B)} = b_e$$

or

$$2B^2 - 3B + \frac{\gamma}{b_e} = 0,$$

where b_e denotes the experimental factor resulting from the bubble growth equation at the instant t_1 of departure. The quadratic equation has a unique solution $B = 0{\cdot}75$ (corresponding to a fixed angle of contact $\alpha = \pi/3$, cf. equation (2) and 1.6) only as $\gamma = \frac{9}{8}b_e$, i.e. the value 0·89 is an upper boundary for b_e, cf. Table 1. For instance, for water $b_e = 0{\cdot}70$, whence $b^* = \frac{9}{8}b_e B = 0{\cdot}59$, and for 4·1 wt. % methylethylketone $b_e = 0{\cdot}895$, whence $\gamma = 1{\cdot}00$ and $b^* = B = 0{\cdot}75$. The generalization of (16) results in a factor $\frac{32}{27}b^*$ instead of the original factor b^* for a sphere (perfect wetting), whence

$$R^* = \tfrac{32}{27}b^* C_1 \vartheta_0 u$$

The volume of the spherical segment amounts to:

$$V_b = \frac{4\pi}{3}B^2(3 - 2B)(R^*)^3 = \frac{4\pi}{3}\tfrac{27}{32}(R^*)^3 = \frac{4\pi}{3}R^3,$$

where the radius R of the equivalent sphere with equal volume is defined by:

$$R = (\tfrac{27}{32})^{\frac{1}{3}}R^* = (\tfrac{32}{27})^{\frac{2}{3}}b^* C_1 \vartheta_0 u = bC_1\vartheta_0 u,$$

i.e. formally, equation (16) again, but with a different meaning of the factor b. In case of a spherical bubble $b = b^*$. For a spherical segment, however, the "bubble growth parameter" b is related to the microlayer parameter b^* according to:

$$b = \frac{b^*}{\{B^2(3 - 2B)\}^{\frac{1}{3}}} = (\tfrac{32}{27})^{\frac{2}{3}}b^* = 1{\cdot}12b^*.$$

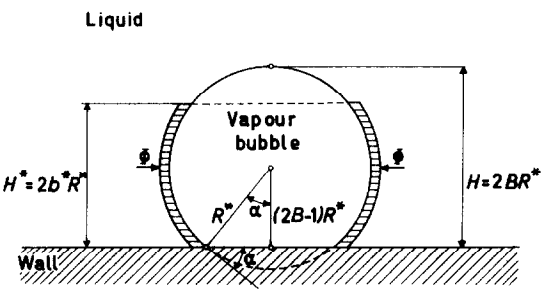

FIG. 5. Partial heat supply to spherical bubble segment.

It is striking that the contact angle occurring during the dynamic bubble growth at a heating surface is predicted to be independent of interfacial tensions, which determine the static behaviour of liquid drops on plates. In fact, however, the numerical value of the parameter b^* is of minor importance in comparison to that of b. A value of $B \neq 0{\cdot}75$, if actually occurring, should result in a different ratio b/b^*. This can be incorporated in the theory by admitting values of the discriminant of the quadratic equation in B, which are > 0.

The area of the spherical bubble segment, through which heat is transmitted to the bubble, amounts to

$$A_2 = 2\pi R^* H^* = 4\pi b^* (R^*)^2 = 4\pi \frac{\{B^2(3-2B)\}^{\frac{2}{3}}}{\{B^2(3-2B)\}^{\frac{2}{3}}} bR^2 = 4\pi bR^2,$$

i.e. exactly the same expression as for a sphere. This justifies the theoretical picture, in which growing bubbles at a heating surface are replaced by free spherical bubbles with partial heat supply.

During the last stage of adherence, the area of contact between the vapour in the bubble space and the heating surface diminishes gradually to zero at the instant of departure, justifying the proposed theoretical picture. Meanwhile, cold liquid of the bulk is already rushing in to the outer part of the contact area, which was previously covered with vapour. This explains why the theoretical ratio of the delay and departure times exceeds the experimental value, cf. Part II. The value of the parameter b in the extension of (16) has been derived from the experimental values $R_{1,e}$ and $u_{1,e} = t_{1,e}^{\frac{1}{2}}$ at the instant $t_{1,e}$ of departure, i.e.

$$b = eR_{1,e}/C_1 \vartheta_0 u_{1,e},$$

cf. Table 1. It is shown that this value of b, which has been determined at one instant only, holds for the whole period of adherence, cf. Fig. 7; i.e. the growth rate of bubbles at a heating surface equals that of free spherical bubbles with corresponding partial heat supply. This statement is even valid for vibrating bubbles, the shape of which is transformed periodically into a rotation ellipsoid (Figs. 4 and 7).

2.4 *Coefficient of heat transfer to a bubble*

The coefficient of heat transfer to a free vapour bubble can be derived from equations (3) and (9):

$$h = \frac{k}{d_b} = \frac{\Phi}{A_1 \vartheta_0} = \frac{\rho_2 l}{\vartheta_0} \frac{\mathrm{d}R}{\mathrm{d}t} = \tfrac{1}{2}\rho_2 l C_1 u^{-1}. \quad (17)$$

This expression holds also in case of partial heat supply as d_b is independent of b.

3. BUBBLE GROWTH FOR TIME-DEPENDENT LIQUID SUPERHEATING

3.1 *Importance for the region of nucleate boiling*

This case is of extreme practical importance, since it occurs actually for vapour bubbles, which are generated at a heating surface in the region of nucleate boiling. Generally, the superheating of the surface ϑ_0 (and the adjacent thermal boundary layer, of which the thickness d_w is of the order of 10^{-5} m = 10 μ) amounts to approximately 10–40 degC. The equilibrium bubble radius R_0 is then approximately 1 μ, whence extremely high initial growth rates are predicted, in good agreement with experimental results [35, 39, 60, 31]. Subsequent bubble growth after release is much slower due to the small (uniform) superheating $\Delta\vartheta_0$ of the bulk liquid, which is of the order of 0·1 degC.

3.2 *The new approach of the mechanism of nucleate boiling*

The formation of vapour bubbles on a nucleus in the region of nucleate boiling (or at the liquid–vapour interface in film boiling) is attributed here to a periodic heating and cooling of a thin liquid microlayer (with height $H^* = 2bR$ and thickness d) of uniform superheating ϑ. Consequently, the theory of relaxation phenomena, which is well-known from mechanical vibrations and electrical circuits, can be applied here to describe the time-dependence of the temperature.

At first sight, Newton's cooling law with the solution

$$\vartheta = \vartheta_0 \exp(-t/\tau), \quad (18)$$

where τ denotes the relaxation time (or time constant), seems to give a suitable starting point. However, the situation is somewhat more complex than in the simple case where Newton's law holds, since both the coefficient of heat transfer, cf. equation (17), and the ratio of the heat capacity of the microlayer to the area of contact surface depend on time here. The height of the superheated microlayer adjacent to the bubble is assumed to increase linearly with the bubble

radius, cf. Section 2.3.2. Consequently, superheated liquid should rise together with the growing bubbles at the wall. This is exactly what is shown in recent shadowgraph studies, cf. Section 1.6.

3.3 *Validity of the bubble growth equation in case of partial heat supply*

A spherical vapour bubble in a superheated liquid is a moving spherical surface heat sink, which can be found by integration of an expanding instantaneous point sink.

The extended Rayleigh equation of motion can be written here, according to Forster and Zuber's [27] derivation of equation (9), cf. also [31]:

$$R\frac{d^2R}{dt^2} + \tfrac{3}{2}\left(\frac{dR}{dt}\right)^2 = -\frac{\rho_2 l}{\rho_1 T}\left\{\frac{\rho_2 l}{(12/\pi)^{\frac{1}{2}}\rho_1 c a^{\frac{1}{2}}} C_2 - \vartheta\right\} - \frac{2\sigma}{\rho_1 R} \quad (19)$$

The hydrodynamic terms in the left-hand side and the last term in the right-hand side of this equation are time-dependent, even for $\vartheta = \vartheta_0 =$ constant. These terms are proportional to t^{-1} and $t^{-\frac{1}{2}}$, respectively, and hence vanish for relatively large time.

At atmospheric boiling point, and e.g. for $\vartheta = \vartheta_0 = 20$ degC, the order of magnitude of the left-hand side is $10^{-1}t^{-1}$ to t^{-1} m^2/s^2, and of the last term in the right-hand side $10t^{-\frac{1}{2}}$ to $10^2 t^{-\frac{1}{2}}$. m^2/s^2. The coefficient of the term between brackets in the right-hand side is then of the order of magnitude of 10^5 to 10^6 m^2/s^2 degC.

Already after a few microseconds, equation (19) can thus be simplified to:

$$C_2 = \left(\frac{12}{\pi}\right)^{\frac{1}{2}} \frac{(k\rho_1 c)^{\frac{1}{2}}}{\rho_2 l}\vartheta = C_1\vartheta, \quad (20)$$

or for partial heat supply:

$$R = bC_2 u = bC_1\vartheta u, \quad (21)$$

i.e. equation (16), provided that ϑ changes relatively slowly with time, such that the first term in the right-hand side of equation (19) remains large in comparison with the other terms. This condition is satisfied here, cf. equation (26).

Equation (16) can also be derived from Scriven's equation [30], which is valid for relatively large superheatings, cf. also [31]:

$$\vartheta = \frac{\rho_2 l}{\rho_1 c}\left(\frac{\pi}{3}\right)^{\frac{1}{2}} \frac{C_2}{2a^{\frac{1}{2}}} = \frac{C_2}{C_1},$$

which yields equation (21).

3.4 *Boundary conditions and temperature of the microlayer*

For the present, the relatively slow subsequent bubble growth after release shall be neglected. As a consequence, the following boundary conditions are introduced:

(1) The coefficient of heat transfer to the bubble $h(t_1) = 0$ at the instant t_1, at which the bubble departs from the heating surface, in good agreement with experimental data, cf. Fig. 7. The departure radius of the bubble is denoted by $R(t_1) = R_1$, and $u_1 = t_1^{\frac{1}{2}}$.

(2) $\vartheta = \vartheta_0$ for $t = 0$, i.e. the initial superheating of the microlayer equals the superheating of the heating surface.

The first condition is equivalent with

$$\left(\frac{dR}{dt}\right)_{t=t_1} = \left(\frac{dR}{du}\right)_{u=u_1} = 0.$$

We assume the validity (for arbitrary u in the interval $0 \leqslant u \leqslant u_1$) of the following expression for the coefficient of heat transfer to the bubble:

$$h(u) = \tfrac{1}{2}\rho_2 l C_1\left(\frac{1}{u} - \frac{1}{u_1}\right). \quad (22)$$

This function satisfies the first boundary condition. The initial values of h are only slightly diminished in comparison to those following from equation (17), since $h(t) \to \infty$ for $t \to 0$.

The superheating of the microlayer $\vartheta(u)$ is determined by equations (22) and (21):

$$h(u) = \tfrac{1}{2}\rho_2 l C_1\left(\frac{1}{u} - \frac{1}{u_1}\right) = \frac{\rho_2 l}{b\vartheta}\frac{dR}{dt} = \frac{\rho_2 l}{b\vartheta}\frac{1}{2u}\frac{dR}{du} = \tfrac{1}{2}\rho_2 l C_1\left(\frac{1}{u} + \frac{1}{\vartheta}\frac{d\vartheta}{du}\right), \quad (23)$$

whence ϑ follows from an ordinary differential equation of the first order:

$$\frac{1}{\vartheta}\frac{\mathrm{d}\vartheta}{\mathrm{d}u} = -\frac{1}{u_1}. \tag{24}$$

The general solution of this equation is

$$\vartheta = D_1 \exp\left(-\frac{u}{u_1}\right). \tag{25}$$

The constant of integration D_1 follows from the second boundary condition, which yields:

$$\vartheta = \vartheta_0 \exp\left(-\frac{u}{u_1}\right). \tag{26}$$

3.5 *Equivalence of equations* (22) *and* (26)

Conversely, assumption of the validity of equation (26) can be shown to be equivalent with the expression (22). Assuming

$$\vartheta = \vartheta_0 \exp(-f_2 u) \tag{27}$$

with f_2 = constant, yields in combination with equation (21)

$$\frac{\mathrm{d}R}{\mathrm{d}u} = bC_1\vartheta(1 - f_2 u), \tag{28}$$

whence

$$h = \frac{\rho_2 l}{b\vartheta}\frac{1}{2u}\frac{\mathrm{d}R}{\mathrm{d}u} = \tfrac{1}{2}\rho_2 l C_1\left(\frac{1}{u} - f_2\right). \tag{29}$$

The first boundary condition yields $f_2 = 1/u_1$, simplifying equation (27) to equation (26).

3.6 *Derivation of the bubble growth equation* (21) *from equations* (27) *and* (29)

The bubble growth equation (21) can also be derived from equations (27) and (29), since

$$h = \tfrac{1}{2}\rho_2 l C_1\left(\frac{1}{u} - f_2\right) = \frac{\rho_2 l}{b\vartheta}\frac{1}{2u}\frac{\mathrm{d}R}{\mathrm{d}u},$$

whence

$$\frac{\mathrm{d}R}{\mathrm{d}u} = bC_1\vartheta_0(1 - f_2 u)\exp(-f_2 u),$$

with $f_2 = 1/u_1$, cf. the first boundary condition.

Integration yields:

$$R = bC_1\vartheta_0 u \exp\left(-\frac{u}{u_1}\right) = bC_1\vartheta u.$$

This means, that each of the three equations for bubble radius, superheating and coefficient of heat transfer, respectively, depends on both remaining ones. However, comparison of theoretical predictions with experimental results can be restricted to bubble growth, since both the superheating of the microlayer and the heat transmission to the bubble are then determined at the same time. The time-dependence of the superheating can be checked separately with Moore and Mesler's and Madsen's curves.

3.7 *Extended Newton's cooling law*

The well-known differential equation for the cooling rate of the microlayer adjacent to a vapour bubble is:

$$-C\frac{\mathrm{d}\vartheta}{\mathrm{d}t} = hA_2\vartheta, \tag{30}$$

where the heat capacity $C = V\rho_1 c$, the volume $V = A_2 d = 4\pi b R^2 d$, and d = thickness of the microlayer.

Hence, equation (30) is simplified here to:

$$-\frac{\mathrm{d}\vartheta}{\mathrm{d}t} = \frac{h}{\rho_1 c d}\vartheta. \tag{31}$$

One can check now the total amount of latent heat of vaporization which is supplied from the cooling microlayer to the vapour bubble during the time of adherence to the heating surface, before the bubble breaks away with a radius R_1 at the instant t_1:

$$\Delta H_0 = \int_0^{t_1} hA_2\vartheta\,\mathrm{d}t = \rho_2 l\int_0^{u_1} 4\pi R^2 bC_1\vartheta_0 \times\left(1 - \frac{u}{u_1}\right)\exp\left(-\frac{u}{u_1}\right)\mathrm{d}u$$

$$= \rho_2 l\int_0^{R_1} 4\pi R^2\,\mathrm{d}R = \frac{4\pi}{3}\rho_2 l R_1^3. \tag{32}$$

Also,

$$\int_0^t hA_2\vartheta \, dt = \frac{4\pi}{3}\rho_2 l R^3$$

for any value of t during adherence, i.e. for $0 \ll t \ll t_1$. Consequently, the instantaneous value of the remaining part of the excess enthalpy (with initial maximal value ΔH_0) stored in the removed relaxation microlayer, amounts to:

$$\Delta H(t) = \Delta H_0 - \frac{4\pi}{3}\rho_2 l R^3 = \frac{4\pi}{3}\rho_2 l(R_1^3 - R^3).$$

3.8 *Thickness of the microlayer*

The thickness of the microlayer follows from equation (31):

$$d = -\frac{h}{\rho_1 c}\frac{\vartheta}{\frac{d\vartheta}{dt}} = \frac{h}{\rho_1 c} 2u\,u_1 = \frac{\rho_2 l}{\rho_1 c} C_1(u_1 - u), \tag{33}$$

whence the maximum value of d, cf. Fig. 6,

$$d_0 = d(0) = \frac{\rho_2 l}{\rho_1 c} C_1 u_1, \tag{34}$$

and

$$d(t_1) = 0.$$

For a pure component

$$d_0 = \left(\frac{12}{\pi}\right)^{\frac{1}{2}} a^{\frac{1}{2}} u_1 \tag{35}$$

The various quantities are shown graphically in Fig. 6.

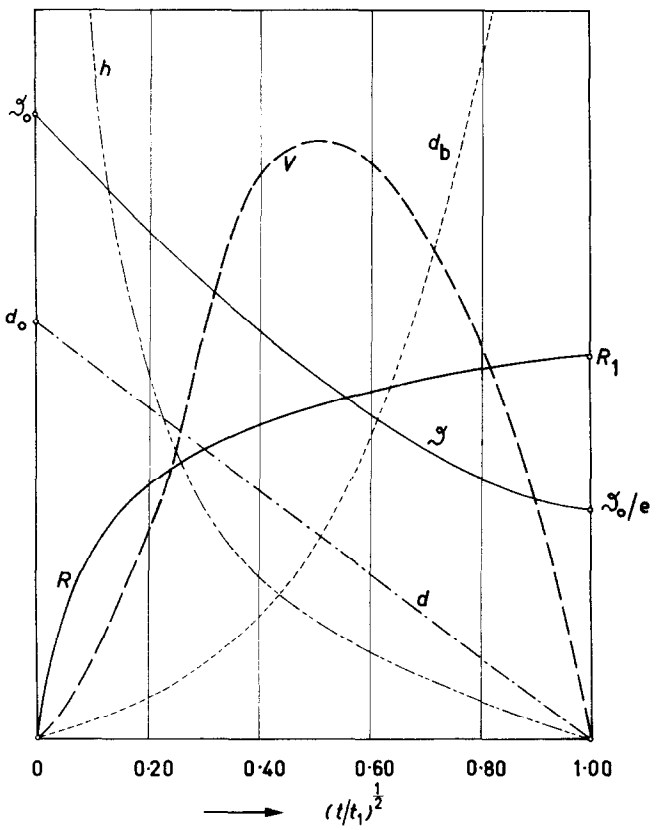

FIG. 6. Bubble radius R, coefficient of heat transfer h to bubble, thickness d_b of equivalent conduction layer around bubble, and superheating ϑ, thickness d and volume V of relaxation microlayer during adherence to heating surface.

3.9 *Volume of microlayer*

The volume of the microlayer (cf. Section 2.3.2) amounts to:

$$V = 4\pi bR^2 d = 4\pi b^3 \frac{\rho_2 l}{\rho_1 c} C_1^3 \vartheta_0^2 \times u^2(u_1 - u) \exp\left(-2\frac{u}{u_1}\right), \quad (36)$$

whence $dV/du = 0$ for $u = 0, u = \frac{1}{2}u_1$ (maximum, cf. Fig. 6) and $u = 2u_1$. The maximum volume of the microlayer occurs for $t = \frac{1}{4}t_1$ (Fig. 6) and amounts to:

$$V_0 = \frac{2\pi}{e} b^3 \frac{\rho_2 l}{\rho_1 c} C_1^3 \vartheta_0^2 u_1^3 = 2\pi b e d_0 R_1^2. \quad (37)$$

3.10 *Thermal boundary layer*

The thickness d_b of the equivalent conduction layer around the vapour bubble is:

$$d_b = \frac{k}{h} = \frac{2k}{\rho_2 l C_1 (1/u - 1/u_1)}, \quad (38)$$

whence $d_b(u) \to \infty$ as $u \to u_1$, cf. Fig. 6. However, this is not disturbing, since the physical meaning is that the temperature gradient at the bubble boundary, which equals ϑ/d_b, vanishes at the instant of release. For free bubbles equation (38) simplifies to:

$$d_b = \frac{2k}{\rho_2 l C_1} u = \left(\frac{\pi}{3}\right)^{\frac{1}{2}} (at)^{\frac{1}{2}}. \quad (39)$$

3.11 *Average values of d and h*

For the purpose of comparing theoretical predictions with Madsen's and Moore and Mesler's values, the average values $\bar{d}$ and $\bar{h}$ are calculated from equations (33) and (22), respectively:

$$\bar{d} = \frac{1}{t_1}\frac{\rho_2 l}{\rho_1 c} C_1 \int_0^{t_1} (t_1^{\frac{1}{2}} - t^{\frac{1}{2}})\, dt = \tfrac{1}{3}\frac{\rho_2 l}{\rho_1 c} C_1 u_1 = \tfrac{1}{3} d_0, \quad (40)$$

and

$$\bar{h} = \frac{1}{2t_1} \rho_2 l C_1 \int_0^{t_1} (t^{-\frac{1}{2}} - t_1^{-\frac{1}{2}})\, dt = \tfrac{1}{2}\rho_2 l C_1 u_1^{-1}. \quad (41)$$

3.12 *Initial bubble growth*

The initial bubble growth follows from equation (21) by taking $t \to 0$, whence:

$$R - R_0 = bC_1 \vartheta_0 u, \quad (42)$$

where the (small) equilibrium radius follows from the Clausius–Clapeyron equation:

$$R_0 = \frac{2\sigma T}{\rho_2 l \vartheta_0} \quad (43)$$

and the initial growth rate

$$\frac{dR}{dt} = \tfrac{1}{2} bC_1 \vartheta_0 u^{-1}. \quad (44)$$

3.13 *Discussion of bubble growth equation* (21)

The bubble radius R_1 at the instant of release is predicted from equation (21) to:

$$R_1 = \frac{b}{e} C_1 \vartheta_0 u_1, \quad (45)$$

whence: (*i*) R_1 increases linearly with the superheating of ϑ_0 of the heating surface in the region of nucleate boiling, if the time t_1 of departure is assumed to be a constant.

(*ii*) R_1 is proportional with the growth constant C_1, i.e. R_1 and C_1 show a minimum at the same concentration of a binary system, if t_1 is independent of concentration, cf. Part II of this paper. This explains the observed coincidence of minimum bubble size, minimum bubble growth and maximum peak flux density in nucleate boiling [31].

(*iii*) Evidently equation (45) shows no preference for any direction, particularly not for gravity. Consequently, previous equations attributing bubble release to equilibrium of buoyancy and the action of surface tension, must be considered to be unreliable. Originally, all bubbles leave the heating surface perpendicularly. Actually vapour bubbles have been observed, in binary mixtures, which leave a horizontal heating wire downwards, cf. Fig. 3.

3.14 *Comparison with previous theory*

A semi-empirical treatment has been given previously by the author [31], predicting for the

bubble radius at the instant of release:

$$R_1 = \frac{1}{n+1} C_1 \vartheta_0 u_1, \qquad (46)$$

where the parameter $n = 3$ for all bubbles generated on "ordinary" nuclei, i.e. independent nuclei at relatively large mutual distances, and $n = 7$ for "complex" nuclei, i.e. nuclei at distances which are of the same order of magnitude as the bubble radius, cf. Section 3.17.

For ordinary nuclei $b = 0{\cdot}70$ whence $b/e = 0{\cdot}26$, which is in accordance with $n = 3$. The reader is referred to Fig. 7 and the original publication [31], where the good agreement of experimental and theoretical values following from equation (46), and hence also from equation (45), is shown for vapour bubbles in water, and in water–methylethylketone and water–1-butanol mixtures.

3.15 *Correction on the bubble growth parameter due to the superheating of the bulk liquid*

As a matter of fact, one has to take instead of equation (21) for growth of bubbles adhering to the heating surface:

$$R = b_1 C_1 \vartheta u + (1 - b_1) C_1 \Delta\vartheta_0 u = b_1 C_1 (\vartheta - \Delta\vartheta_0) u + C_1 \Delta\vartheta_0 u,$$

where $\Delta\vartheta_0$ denotes the constant superheating of the bulk liquid, and

$$\vartheta = \vartheta_0 \exp\left(-\frac{u}{u_1}\right).$$

Consequently,

$$R_1 = \frac{b_1}{e} C_1 \vartheta_0 u_1 + (1 - b_1) C_1 \Delta\vartheta_0 u_1 = C_1 u_1 \left\{\frac{b_1}{e} \vartheta_0 + (1 - b_1)\Delta\vartheta_0\right\}. \qquad (47)$$

It is seen from equations (45) and (47) that

$$b = b_1 + e(1 - b_1)\frac{\Delta\vartheta_0}{\vartheta_0}. \qquad (48)$$

In general, the values of b and b_1 differ only slightly, since $\Delta\vartheta_0 \ll \vartheta_0$; e.g. for $\vartheta_0 = 20$ degC, $\Delta\vartheta_0 = 0{\cdot}3$ degC and $b = 0{\cdot}700$, one has $b_1 = 0{\cdot}687$, i.e. a correction of not more than 2 per cent which can be left out of consideration.

3.16 *Comparison with experiment for some vapour bubbles in water*

A comparison of the theoretical value following from equation (45) by taking $R_{1,t} = R_{1,e}$ yields: $b = 0{\cdot}70$ for water, cf. Table 1. This proves the validity of the assumption, that an updraught of hot liquid adjacent to the bubble boundary is occurring during the time of adherence to the heating surface; the major part $4\pi bR^2$ of the total bubble area $4\pi R^2$ is surrounded by the superheated microlayer, which is cooling rapidly during bubble growth.

The agreement between theoretical and experimental growth during adherence is also excellent, cf. Fig. 7, even better than with the equation derived previously [31].

This means, that the assumption of the validity of equation (26) for the superheating of the microlayer is justified. Hence, the same value $b = 0{\cdot}70$, which is obtained by making a comparison at the instant of release t_1 is also valid during the whole time of adherence. The height $H^* = 2bR$ of the microlayer is increasing then proportionally with the bubble radius.

Hospeti and Mesler [80] observed an increase of R_1 with ϑ_0, which is also predicted by theory, equation (45), for vapour bubbles on a heating surface in water. However, quantitative information has not yet been presented. The author's future research includes experiments on the same subject, for various pure liquids and binary mixtures boiling at different pressures.

3.17 *Complex nuclei*

It has been shown previously [31], that a distinction has to be made between "ordinary" and "complex" nuclei, the mutual distance between the latter being of the same order of magnitude as the bubble size at departure. A high local density occurs of small bubbles generated at very high frequencies on complex nuclei in certain binary mixtures only (Section

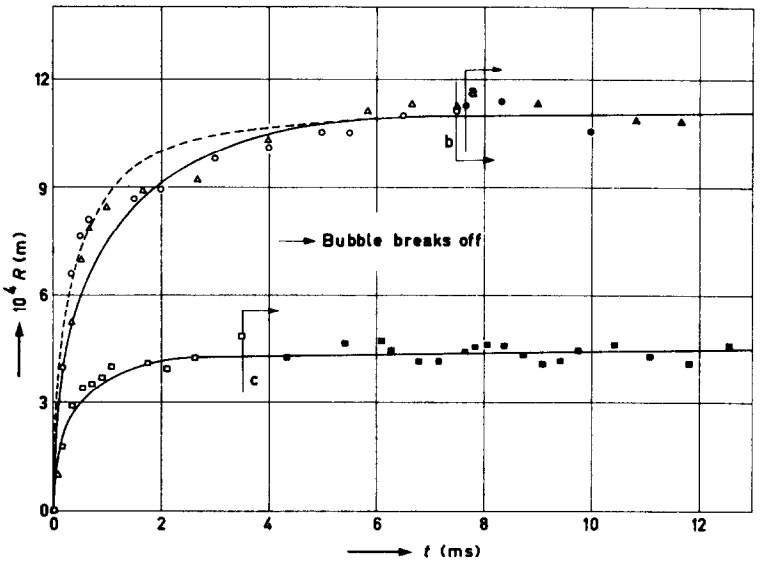

FIG. 7. *Water.* Theoretical growth curves during adherence according to equations (21) and (26):

$$R = bC_1\vartheta_0 t^{\frac{1}{2}} \exp -(t/t_1)^{\frac{1}{2}}$$

and according to previous theory [31]:

$$R = 0{\cdot}25C_1(\varphi_0 - \Delta\varphi_0)[1 - \{1 - (t/l_1)^{\frac{1}{2}}\}^4]t_l^{\frac{1}{2}} + C_1\Delta\varphi_0 t^{\frac{1}{2}} \text{ (- - -)}$$

in comparison to experimental data for bubbles *a* (○, ●) and *b* (△, ▲) with $\vartheta_0 = 20$ degC and $\Delta\vartheta_0 = 0{\cdot}36$ degC and bubble *c* (□, ■) with $\vartheta_0 = 12$ degC and $\Delta\vartheta_0 = 0{\cdot}11$ degC, cf. Table 1.
The subsequent growth after departure follows from : $R = R_1 + C_1\Delta\vartheta_0(t^{\frac{1}{2}} - t_l^{\frac{1}{2}})$.

1.5). Bubble growth during adherence on complex nuclei can obviously be described by reducing the growth constant to half its normal value, i.e. by taking:

$$C_{1,c} = 0{\cdot}50C_{1,m}. \tag{49}$$

This relation follows from the geometrical pattern, showing that each bubble boundary has a neighbouring liquid–vapour interface of equal area with competitive consumption of the more volatile component.

Apparently, the reduction in bubble growth rate on complex nuclei can also be attributed to a decrease in local superheating ϑ_0, which is lowered continuously due to the action of neighbouring bubbles, cf. equations (9) and (12). Formally, one has to replace ϑ_0 then by the average value for an individual bubble:

$$\bar{\vartheta} = \frac{1}{t_1}\int_0^{t_1} \vartheta \, dt = 2\frac{\vartheta_0}{t_1}\int_0^{u_1} u \exp\left(-\frac{u}{u_1}\right) du = \left(2\ 1 - \frac{2}{e}\right)\vartheta_0 = 0{\cdot}53\vartheta_0 \tag{50}$$

$\bar{\vartheta}$ is independent of t_1 and has obviously the same value for all complex nuclei. The growth parameter $b = 0{\cdot}68$ for complex nuclei (Table 1), whence the factor $2(1 - 2/e)b/e$ in the right-hand side of equation (45) is then 0·132, which is in good agreement with the previous value 0·125, cf. [31].

Thus the special behaviour of complex nuclei with decreased bubble growth can be explained satisfactorily both in terms of mass and heat diffusion.

3.18 *The wetting constant*

The value of b is obtained from equation (45) by substitution of the experimental values $t_{1,e}$ and $R_{1,e}$. The same value of b holds for the entire initial stage of growth of adhering bubbles, cf. Section 3.16 and Fig. 7.

The instantaneous height of the removed microlayer amounts to $2bR$ and thus to $2bR_1$ at the instant t_1 of bubble release. The values of the wetting parameter b are shown in Table 1 (cf. Appendix). The average values are: 0·70 for water, 0·73 for all (14) bubbles investigated on ordinary nuclei, 0·68 for complex nuclei and 0·72 for both types of nuclei. The appendix gives also data for bubbles in ethanol, both in nucleate boiling and film boiling.

3.19 *Comparison of the thickness of the microlayer and the coefficient of heat transfer with Madsen's data* [49]

The average values $\bar{d}$ and $\bar{h}$, which have been derived from equations (40) and (41) respectively, are also shown in Table 1. For water $\bar{d} = 21$ μ, in good agreement with Madsen's value of 26 μ, and $\bar{h} = 2{\cdot}09 \times 10^4$ W/m² degC for heat transmission to the bubble. Madsen's value for heat transmission from the surface is higher: $h_w = 3{\cdot}03 \times 10^4$ W/m² degC. Madsen's values are obtained from equation (18) by taking a constant local surface coefficient of heat transfer h_w and a constant relaxation time $\tau = \rho_1 c\bar{d}/h_w$ in Newton's law.

REFERENCES

1. F. S. PRAMUK and J. W. WESTWATER, Effect of agitation on the critical temperature difference for a boiling liquid, *Chem. Engng Prog. Symp. Ser. No. 18*, **52**, 79–83 (1956).
2. S. NUKIYAMA, Maximum and minimum values of heat transmission from metal to boiling water under atmospheric pressure, *Soc. Mech. Japan* **37**, 367–374 (1934); 553–554 (1934).
3. W. R. VAN WIJK and S. J. D. VAN STRALEN, Warmteoverdracht aan kokende binaire vloeistofmengsels (I), *Ned. Tijdschr. Natuurk.* **29**, 287–315 (1963). In Dutch.
4. W. R. VAN WIJK and S. J. D. VAN STRALEN, Warmteoverdracht aan kokende binaire vloeistofmengsels (II), *Ned. Natuurk.* **30**, 116–137 (1964). In Dutch.
5. W. R. VAN WIJK and S. J. D. VAN STRALEN, Maximale Wärmeströmdichte und Wachstumsgeschwindigkeit von Dampfblasen in siedenden Zweistoffgemischen, *Chemie-Ingr-Tech.* **37**, 509–517 (1965).
6. J. L. SCHWEPPE and A. S. FOUST, Effect of forced circulation rate on boiling–heat transfer on pressure drop in a short vertical tube, *Chem. Engng Prog. Symp. Ser. No. 5*, **49**, 77–89 (1953).
7. W. H. MCADAMS, W. E. KENNEL, C. S. MINDEN, R. CARL, P. M. PICORNELL and J. E. DEW, Heat transfer at high rates to water with surface boiling, *Ind. Engng Chem.* **41**, 1945–1953 (1949).
8. W. H. MCADAMS, *Heat Transmission*, 3rd edn. McGraw-Hill, New York (1945).
9. F. KREITH and M. SUMMERFIELD, Heat transfer to water at high flux densities with and without surface boiling, *Trans. Am. Soc. Mech. Engrs* **71**, 805–815 (1949). Pressure drop and convective heat transfer with surface boiling at high heat-flux, data for aniline and *n*-butyl alcohol, *Trans. Am. Soc. Mech. Engrs* **72**, 869–879 (1950).
10. F. C. GUNTHER, Photographic study of surface boiling heat transfer to water with forced convection, *Trans. Am. Soc. Mech. Engrs* **73**, 115–123 (1951).
11. W. R. GAMBILL and N. D. GREENE, Boiling burnout with water in vortex flow, *Chem. Engng Prog. No. 10*, **54**, 68–76 (1958).
12. H. SENFTLEBEN, Die Einwirkung elektrischer und magnetischer Felder auf das Wärmeleitvermögen von Gasen, *Phys. Z.* **32**, 550 (1931). Zur Frage der Deutung des Einflusses elektrischer Felder auf den Wärmestrom in Gasen, *Phys. Z.* **35**, 661–662 (1934).
13. E. BONJOUR, J. VERDIER and L. WEIL, Compte rendu des septièmes journées de l'hydraulique Paris, 1962; Société hydrotechnique de France, Paris (1962).
14. E. A. FARBER and R. L. SCORAH, Heat transfer to water boiling under pressure, *Trans. Am. Soc. Mech. Engrs* **70**, 369–384 (1948).
15. S. J. D. VAN STRALEN, Warmteoverdracht aan kokende binaire vloeistofmengsels, Doctor thesis, Univ. of Groningen, Netherlands; Veenman, Wageningen, Netherlands (1959); *Meded. LandbHoogesch. Wageningen* **59** (6) (1959). In Dutch with English summary and captions.
16. E. K. AVERIN, The effect of roughness of the heating surface on the heat transfer to water boiling under atmospheric pressure, *Izv. Akad. Nauk SSSR, Otdel. Tekh. Nauk* (3), 116–122 (1954); *De Ingenieur* **60**, Ch. 64 (1957). Translated by Associated Technical Services: Translations R.J.-305.
17. M. T. CICHELLI and C. F. BONILLA, Heat transfer to liquids boiling under pressure, *A.J.Ch. Jl* **41**, 755–787 (1945).
18. J. N. ADDOMS, Heat transfer at high rates to water boiling outside cylinders, Sc.D. thesis in chemical engineering, Massachusetts Inst. Technology (1948).
19. S. J. D. VAN STRALEN, Heat transfer to boiling binary liquid mixtures, *Br. Chem. Engng* **4**, 8–17 (1959); **4**, 78–82 (1959); **6**, 834–840 (1961); **7**, 90–97 (1962).
20. E. A. KAZAKOVA, The maximum heat transfer to boiling water at high pressure, *Izv. Akad. Nauk SSSR, Otdel.*

Tekh. Nauk (1), 1377–1387 (1950); *Eng. Digest* **12**, 81–85 (1951).
21. A. S. Vos and S. J. D. van Stralen, Heat transfer to boiling water–methylethylketone mixtures, *Chem. Engng Sci.* **5**, 50–56 (1956).
22. W. R. van Wijk, A. S. Vos and S. J. D. van Stralen, Heat transfer to boiling binary liquid mixtures, *Chem. Engng Sci.* **5**, 68–80 (1956).
23. S. J. D. van Stralen, Heat transfer to boiling binary liquid mixtures at atmospheric and subatmospheric pressures, *Chem. Engng Sci.* **5**, 290–296 (1956).
24. W. R. van Wijk, Wärmeübertragung an siedenden Zweistoffgemischen, *Dechema-Monogr.* **28**, 63–74 (1956).
25. W. R. van Wijk and S. J. D. van Stralen, Wärmeübertragung an siedenden Zweistoffgemischen II, *Dechema-Monogr.* **32**, 94–106 (1959).
26. M. Carne, Studies of the critical heat-flux for some binary mixtures, *Can. J. Engng* **41**, 235–241 (1963).
27. H. K. Forster and N. Zuber, Growth of a vapor bubble in superheated liquid, *J. Appl. Phys.* **25**, 474–478 (1953); Conference on nuclear engineering, Univ. of California, Los Angeles (1955).
28. M. S. Plesset and S. A. Zwick, The growth of vapor bubbles in superheated liquids, *J. Appl. Phys.* **25**, 493–500 (1954).
29. P. J. Bruijn, On the asymptotic growth rate of vapour bubbles in superheated binary liquid mixtures, *Physica, 's Grav.* **26**, 326–334 (1960).
30. L. E. Scriven, On the dynamics of phase growth, *Chem. Engng Sci.* **10**, 1–13 (1959).
31. S. J. D. van Stralen, The growth rate of vapour bubbles in superheated pure liquids and in binary mixtures, Parts I–IV, accepted for publication in *Br. Chem. Engng* **11** (1966); **12** (1967).
32. M. Jakob, *Heat Transfer*, Vol. 1. Wiley, New York, Chapman & Hall, London (1950).
33. M. Jakob, Heat transfer in evaporation and condensation, *Mech. Engng* **58**, 643–660, 729–739 (1936).
34. P. J. Dergarabedian, The rate of growth of vapour bubbles in superheated water, *J. Appl. Mech.* **20**, 537–545 (1963).
35. W. R. van Wijk and S. J. D. van Stralen, Growth rate of vapour bubbles in water and in a binary mixture boiling at atmospheric pressure, *Physica, 's Grav.* **28**, 150–171 (1962).
36. W. Wanninger, Über die Dynamik von Dampfblasen in Propan, Doctor thesis, Technische Hochschule, Stuttgart, Germany (1964).
37. W. Fritz, Grundlagen der Wärmeübertragung beim Verdampfen von Flüssigkeiten, *Chemie-Ingr-Tech.* **35**, 753–764 (1963).
38. J. E. Benjamin and J. W. Westwater, Bubble growth in nucleate boiling of a binary mixture, Prepr. International heat transfer conference, Boulder, Colorado (1961).
39. S. J. D. van Stralen, Growth rate of vapour bubbles in water–1-butanol mixtures boiling at atmospheric pressure, *Physica, 's Grav.* **29**, 602–616 (1963).
40. Y. Y. Hsu, On the size range of active nucleation cavities on a heating surface, *J. Heat Transfer* **84**, 207–219 (1962).
41. Y. Y. Hsu and R. W. Graham, An analytical and experimental study of the thermal boundary layer and ebullition cycle in nucleate boiling, NASA Resp. TN-D-594 (1961).
42. G. Leppert and C. C. Pitts, Boiling, in *Advances in Heat Transfer*, Vol. 1. Academic Press, New York, London (1964).
43. M. Béhar and R. Séméria, The use of strioscopic observation methods in boiling and de-aeration studies, *Houille Blanche* **6**, 687–691 (1963).
44. H. Brauer, Schlierenoptische Beobachtung bei der Wärmeübertragung, *Chemie-Ingr-Tech.* **34**, 73–78 (1962).
45. D. A. Bendersky, A special thermocouple for measuring transient temperatures, *Mech. Engng* **75**, 117–121 (1953).
46. F. D. Moore and R. B. Mesler, The measurement of rapid surface temperature fluctuations during nucleate boiling of water, *A.I.Ch.E. Jl* **7**, 620–624 (1961).
47. N. Madsen and C. F. Bonilla, Heat transfer to sodium-potassium alloy in pool boiling, *Chem. Engng Prog. Symp. Ser. No.* 30, **56**, 251–259 (1960).
48. T. F. Rogers and R. B. Mesler, An experimental study of surface cooling by bubbles during nucleate boiling of water, *A.I.Ch.E. Jl* **10**, 656–660 (1964).
49. N. Madsen, Temperature fluctuations at a heated surface supporting pool boiling of water, Lab. Rep., Lab. of heat transfer and reactor engineering, Technological Univ. of Eindhoven, Netherlands (1964); Symposium on boiling heat transfer in steam-generated units and heat exchangers, Manchester, Paper No. 14 (1965), to be published in *Proc. Instn Mech. Engrs* **180** (3C) (1965–66).
50. C. Bonnet, E. Macke and R. Morin, Visualisation de l'ébullition nuclée de l'eau a pression atmosphérique et mesure simultanée des variations de température de surface, Euratom Rep. Eur 1622.f (1964), Centre Commun de Recherche Nucleaire, Etablissement d'Ispra—Italië.
51. K. Stephan, Mechanismus und Modellgesetz des Wärmeübergangs bei der Blasenverdampfung, *Chemie-Ingr-Tech.* **35**, 775–778 (1963).
52. K. Stephan, Beitrag zur Thermodynamik des Wärmeüberganges beim Sieden, Doctor thesis, Technische Hochschule, Karlsruhe; Müller, Karlsruhe (1964).
53. W. Kast, Bedeutung der Keimbildung und der instationären Wärmeübertragung für den Wärmeübergang bei Blasenverdampfung und Tropfenkondensation, *Chemie-Ingr-Tech.* **36**, 933–940 (1964).
54. H. Gröber, S. Erk and U. Grigull, *Die Grundgesetze der Wärmeübertragung*, 3rd edn. Springer, Berlin/Göttingen/Heidelberg (1955).
55. C. Y. Han, Mechanism of heat transfer in nucleate pool boiling, Sc.D. thesis, Mech. Engng Dept., Massachusetts Inst. of Technology (1962).
56. W. M. Rohsenow, *Developments in Heat Transfer*, Ch. 8. M.I.T. Press, Massachusetts Institute of Technology, Cambridge, Massachusetts (1964).
57. J. L. Hudson and S. G. Bankoff, An exact solution of unsteady heat transfer to a shear flow, *Chem. Engng Sci.* **19**, 591–598 (1964).
58. H. S. Carslaw and J. C. Jaeger, *Conduction of Heat in Solids*, 2nd edn. Oxford Univ. Press, Oxford (1959).
59. C. J. Rallis and H. H. Jawurek, Latent heat transport

in saturated nucleate boiling, *Int. J. Heat Mass Transfer* **7**, 1051–1068 (1964).
60. S. J. D. VAN STRALEN, *6th International Congress on High-speed Photography 1962*, pp. 534–539. Scheveningen, Netherlands; Tjeenk Willink, Haarlem, Netherlands (1963).
61. R. F. GAERTNER, Photographic study of nucleate pool boiling on a horizontal surface, Research Lab. Prepr. 5181, Gen. Elect. Co., Schenectady, New York.
62. N. ZUBER, Recent trends in boiling heat transfer research—Part 1: Nucleate pool boiling, *Appl. Mech. Rev.* **7**, 633–672 (1964); Nucleate boiling. The region of isolated bubbles and the similarity with natural convection, *Int. J. Heat Mass Transfer* **6**, 53–78 (1963).
63. J. HOVESTREIJDT, The influence of the surface tension difference on the boiling of mixtures, *Chem. Engng Sci.* **18**, 631–639 (1963).
64. W. M. ROHSENOW, Heat transfer with evaporation, in *Heat Transfer Symposium*, Univ. of Michigan (1953).
65. S. S. KUTATELADZE, Hydrodynamic theory of changes in the boiling process under free convection conditions, *Izv. Akad. Nauk SSSR, Otdel Tekh. Nauk* (4), 529–536 (1951).
66. N. ZUBER, On the stability of boiling heat transfer, *Trans. Am. Soc. Mech. Engrs* **80**, 711–720 (1958).
67. N. ZUBER and M. TRIBUS, Further remarks on the stability of boiling heat transfer, Rep. 58-5, Dept. of Engng, Univ. of California, Los Angeles (1958).
68. U. GRIGULL, Private communication (1962).
69. J. W. WESTWATER and J. G. SANTANGELO, Photographic study of boiling (High speed motion picture), Univ. of Illinois, Urbana (1954); *Ind. Engng Chem.* **47**, 1605–1610 (1955).
70. J. W. WESTWATER, Boiling of liquids, in *Advances in Chemical Engineering*, Vols. 1, 2. Academic Press, New York (1956, 1958).
71. J. W. WESTWATER, Measurements of bubble growth during mass transfer, in *Cavitation in Real Liquids*. Elsevier, Amsterdam (1964).
72. S. J. D. VAN STRALEN, High speed motion picture, Agric. Univ., Wageningen, Netherlands (1960).
73. M. VOLMER and H. FLOOD, Tröpfchenbildung in Dämpfen, *Z. Phys. Chem.* (A), **170**, 273–285 (1934).
74. H. FLOOD, Tröpfchenbildung in übersattigten Äthylalkohol–Wasserdampfgemischen, *Z. Phys. Chem.* (A), **170**, 286–294 (1934).
75. M. VOLMER, *Kinetik der Phasenbildung*. Steinkopf, Dresden/Leipzig (1939).
76. J. A. FROEMKE, C. R. BLOOMQUIST and E. X. ANDERSON, Die Kernbildung kondensierter Dämpfe in nichtionisierter staubfreier Luft (II). Das System Methylalkohol–Wasser, *Z. Phys. Chem.* (A) **166**, 305–315 (1933).
77. F. BOŠNJAKOVIĆ, Verdampfung und Flüssigkeitsüberhitzung, *Tech. Mechanik Thermo-dynam.* **1**, 358–362 (1930).
78. W. PRÜGER, Die Verdampfungsgeschwindigkeit von Flüssigkeiten, *Z. Phys.* **115**, 202–244 (1940); *Forsch. Geb. IngWes.* **12**, 258–260 (1941).
79. N. B. DONALD and F. HASLAM, The mechanism of the transition from nucleate to filmboiling, *Chem. Engng Sci.* **8**, 287–294 (1958).
80. N. B. HOSPETI and R. B. MESLER, A high speed motion picture study of surface temperature changes occurring during bubble growth in nucleate boiling of water, *7th International Congress on High-speed Photography 1965*, Preprint 35. Zürich, Switzerland (1965).

APPENDIX

Experimental data on bubble growth at a horizontal platinum heating wire (with a diameter $D_w = 2 \times 10^{-4}$ m) are shown in Table 1 for a constant heat flux density $q_w = 45 \times 10^4$ W/m^2, which means a moderate value in the region of nucleate boiling. The maximum microlayer superheating for complex nuclei has been replaced by the average value according to equation (50).

The various bubbles are denoted with the same letters as used in previous articles [31], where a number of figures and photographs is showing bubble growth, cf. also Figs. 3 and 4.

The average thickness $\bar{d} = \frac{1}{3}d_0$ of the microlayer amounts to: 21·1 μ in water, 5·5 μ in 4·1 wt. % methylethylketone, 13·0 μ in 1·5 wt. % and 8·6 μ in 6·0 wt. % 1-butanol.

The wetting parameter b is a constant during the entire time of adherence to the heating surface (Fig. 7), and amounts to 0·70 for bubbles in water, 0·73 for ordinary nuclei, 0·68 for complex nuclei and 0·72 for all bubbles investigated, whence the factor $b/e = 0{\cdot}26$ in equation (45).

The average value $\bar{h}$ of the coefficient of heat transfer to the bubble is: $2{\cdot}09 \times 10^4$ W/m^2 degC in water, $0{\cdot}47 \times 10^4$ W/m^2 degC in 4·1 wt. % methylethylketone, $2{\cdot}03 \times 10^4$ W/m^2 degC in 1·5 wt. % and $4{\cdot}19 \times 10^4$ W/m^2 degC in 6·0 wt. % 1-butanol.

The quantity $\overline{h\vartheta}$ is a measure for the heat flux density towards the bubble boundary during adherence. However, relatively large values for complex nuclei correspond with relatively low values of the rate of heat flow Φ due to the small bubble size, cf. the last column.

Some vapour bubbles have tentatively been studied in ethanol, both in the regions of nucleate boiling and film boiling. A coincidence of a small bubble growth constant ($C_1 = 9 \times 10^{-4}$ m/s$^{\frac{1}{2}}$

Table 1

Liquid	Bubble	ϑ_0 (degC)	$10^2 t_{1,e}^{\dagger}$ ($s^{\frac{1}{2}}$)	$10^4 R_{1,e}$ (m)	b_e	$\vartheta_0(1-1/e)$ (degC)	$\bar{d}$ (μ)	d_0 (μ)	$10^{-4}\bar{h}\bar{\vartheta}$ (W/m^2)	$10^{-4}\bar{h}$ (W/m^2 degC)	$\bar{h}t_1$ (J/m^2 degC)	$\bar{\vartheta}$ (degC)	$\bar{h}\bar{\vartheta}t_1$ (J/m^2)	$(4\pi/3)\,10^6\rho_2 l R_1^3$ (J)
Ordinary nuclei														
water	*a*	20	8·75	11·0	0·71	14	23·4	70·1	19·60	1·851	141·5	10·6	1499	7537
$C_1 = 24 \times 10^{-4}$	*b*	20	8·65	11·0	0·72	14	23·1	69·3	19·85	1·872	139·8	10·6	1482	7537
$m/s^{\frac{1}{2}}$ degC	*e*	20	8·15	10·0	0·69	14	21·8	65·3	22·02	1·985	131·9	10·6	1398	5561
	c	12	6·00	4·4	0·69	9	16·0	48·0	17·04	2·696	97·1	6·3	611	481
	d	17	7·85	8·4	0·71	12	21·0	63·0	18·55	2·060	126·9	9·0	1143	3354
4·1% methylethylketone	*a*	24	8·65	4·3	0·93	17	5·7	17·2	5·74	0·452	33·9	12·7	431	435
$C_1 = 6 \times 10^{-4}$	*b*	24	8·10	3·7	0·86	17	5·4	16·1	6·11	0·482	31·8	12·7	406	227
$m/s^{\frac{1}{2}}$ degC														
1·5% 1-butanol	*a*	21	7·25	8·1	0·80	15	14·5	43·5	18·26	1·645	86·7	11·1	962	2960
$C_1 = 18 \times 10^{-4}$	*b*	21	7·00	7·0	0·72	15	14·0	42·0	18·93	1·704	83·7	11·1	930	1909
$m/s^{\frac{1}{2}}$ degC	*c*	21	7·40	7·7	0·75	15	14·8	44·4	17·88	1·612	88·3	11·1	980	2542
	d	21	7·20	7·1	0·71	15	14·4	43·2	18·42	1·658	85·8	11·1	955	1993
	e	21	10·70	8·8	0·59	15	21·4	64·2	12·39	1·118	127·7	11·1	1419	3793
	f	21	4·65	4·5	0·70	15	9·3	27·9	28·47	2·567	55·7	11·1	620	507
	g	7	3·65	1·1	0·65	5	7·3	21·9	12·10	3·270	43·5	3·7	159	7·5
Complex nuclei														
1·5% 1-butanol	*h*	11	4·25	2·0	0·65	8	8·5	25·5	16·29	2·809	50·7	5·8	293	44
6·0% 1-butanol	*a*	11·5	3·40	2·0	0·66	8	7·9	23·7	24·28	3·982	46·1	6·1	281	43
$C_1 = 21 \times 10^{-4}$	*b*	11·5	4·25	2·6	0·69	8	9·9	29·7	19·43	3·186	57·4	6·1	352	95
$m/s^{\frac{1}{2}}$ degC	*c*	11·5	5·30	3·7	0·79	8	12·3	37·0	15·58	2·554	71·6	6·1	435	274
	d	11·5	3·65	2·2	0·67	8	8·5	25·5	22·61	3·710	49·4	6·1	301	58
	e	11·5	1·80	1·0	0·63	8	4·2	12·6	45·90	7·520	24·7	6·1	147	5·4

degC) and a relatively low peak flux density in nucleate boiling ($q_{w,max} = 46 \times 10^4$ W/m^2) occurs in this pure liquid, in contrast to the investigated 4·1 wt. % methylethylketone mixture (6×10^{-4} m/s$^{\frac{1}{2}}$ degC and 172×10^4 W/m^2, respectively). The bubbles are becoming hemispherical for increasing wire-superheating in agreement with Hospeti and Mesler [80], i.e. $b = 0{\cdot}50$ was found in film boiling at $\vartheta_{0,w} =$ 290 degC and at an initial superheating of the liquid microlayer of approximately 90 degC, corresponding with a vapour film of 18 μ. This value of the microlayer superheating is in accordance with Madsen's temperature dips up to 75 degC in film boiling and is connected with a large bubble radius at departure (23×10^{-4} m in comparison to 3×10^{-4} m for nucleate boiling).

Résumé—Notre modification des théories de Van Wijk, Vos et van Stralen, de Scriven et de Bruijn concernant la vitesse de croissance de bulles de vapeur, sphériques libres dans des mélanges binaires surchauffés uniformément a été étendue aux cas plus complexes des bulles produites sur une paroi chauffénte avec une surchauffe du liquide dépendant du temps, conduisant à une nouvelle description du mécanisme de l'ébullition nucléée.

Le flux de chaleur vers la bulle nécessaire pour la vaporisation pendant la croissance rapide initiale de la bulle a été obtenu à partir de l'enthalpie en excédent de la couche limite de conduction équivalente sur la paroi chauffante. Cette couche limite thermique est périodiquement détachée de la paroi à cause de la production successive de bulles sur les noyaux d'ébullition. On a constaté la similitude du comportement de la surchauffe uniforme de la microcouche fluctuante avec un phénomène de relaxation.

Les différentes interprétations des chutes rapides de température à la paroi chauffante, qui se produisent à la fois dans l'ébullition nucléée et l'ébullition par film et qui sont dues à la formation initiale de vapeur ont été discutées et on a également vérifié le mécanisme proposé avec des strioscopies provenant de la littérature.

La croissance expérimentale des bulles adhérant à un fil chauffant en platine dans l'eau, et dans des mélanges eau–méthyléthylcétone et eau–1-butanol, est en accord quantitatif avec la nouvelle théorie.

Zusammenfassung—Die Modifizierung der Theorien von van Wijk, Vos und van Stralen, von Scriven und von Bruijn, die die Wachstrumsgeschwindigkeit von freien, kugelförmigen Dampfblasen in einer gleichförmig überhitzten Zweistoffmischung behandeln, wird durch den Autor auf den komplexeren Fall der Blasenerzeugung an einer Heizfläche und einer zeitabhängigen Flüssigkeitsüberhitzung ausgedehnt. Das führt zu einer neuen Beschreibung der Vorgänge beim Blasensieden.

Der für die Verdampfung bej schnellem Blasenanfangswachstum nötige Wärmestrom in die Blase wurde aus der Überschussenthalpie der äquivalenten, leitenden Schicht an der Heizfläche abgeleitet. Diese thermische Grenzschicht wird von der Wand wegan des aufeinanderfolgenden Entstehens der Blasen an den Keimstellen periodisch weggestossen. Das Verhalten der gleichförmigen Überhitzung in der fluktuierenden Mikroschicht wird ähnlich wie ein Relaxationsphänomen festgelgt.

Die verschiedenen Auslegungen der schnellen Temperaturerniedrigungen an der Heizfläche, die sowohl beim Blasen-wie auch beim Filmsieden auf Grund der anfänglichen Dampfbildung auftreten, wurden diskutiert und der vorgeschlagene angeführte Mechanismus wurde mit Schlierenaufnahmen aus dem Schrifttum überprüft.

Das experimentell bestimmte Wachstum von Blasen, die einem Heizdraht aus Platin in Wasser, in Wasser–Methyl-Ethylketon- und in Wasser–1-Butanolgemischen anhaften, stimmt quantitativ mit der neuen Theorie überein.

Аннотация—Автором внесены изменения в теории Ван Вийка, Воса и Ван Штралена, Скривена и Брюйна роста свободных сферических пузырьков пара в однородно-перегретых бинарных смесях. Эти концепции развиты на более сложные случаи образования пузырьков на поверхности нагрева и перегрева жидкости с течением времени, что привело к новому описанию механизма пузырькового кипения.

Количество тепла, необходимого для испарения в период быстрого начального роста пузырьков, подсчитывается по избыточной энтальпии эквивалентного проводящего слоя на поверхности нагрева. Этот тепловой пограничный слой периодически отодвигается от стенки из-за образования очередных пузырьков на ядрах. Установлено, что картина однородного перегрева пульсирующего микрослоя подобна явлению релаксации.

Дается различная интерпретация быстрых снижений температуры, происходящих на поверхности кипения как при пузырьковом, так и при пленочном кипении из-за начального парообразования. Предложенный механизм проверен оптическим методом полос по фотографиям, заимствованным из литературы.

Экспериментальные данные о росте пузырьков, прилипающих к платиновой нагреваемой проволоке в воде и смесях вода–метилэтилкетон и вода–1–бутанол, находятся в количественном согласии с новой теорией.